(i) Title:

Hallucination- and delusion-like experiences are associated with increased precision of sensory evidence in perceptual inference

(ii) Running title:

Hallucination- and delusion-like experiences are associated with increased precision of sensory evidence in perceptual inference

(iii) Authors:

Francesco Scaramozzino
Royal Holloway, University of London

Ryan McKay
Royal Holloway, University of London

Nicholas Furl
Royal Holloway, University of London

(iv) Corresponding author:
Francesco Scaramozzino;
Egham Hill, Egham TW20 0EQ, UK;
+441784276884
francesco.scaramozzino@rhul.ac.uk

(v) Word count:
Abstract:
Text body:

Abstract

BACKGROUND AND HYPOTHESIS. Predictive coding proposes that psychotic phenomenology stems from alterations in precision encoding of neural signals. Previous studies indicate links between psychotic-like experiences, increased sensory evidence precision, and reduced data-gathering in probabilistic reasoning. If sensory precison is increased in bottom-up signalling, we would expect it to be present in perceptual inference. Here, we investigated whether increased sensory precision and reduced data-gathering relate to subclinical psychotic-like experiences in perceptual inference.

STUDY DESIGN. We fitted drift-diffusion models to performance on the Random Dot Motion task (RDM) of 191 participants from the general population. Drift rate (a proxy for precision of sensory evidence) and decision threshold parameters could vary: 1) between groups with higher vs. lower levels of psychotic phenotypes; 2) as dependent variables in a regression model having psychotic phenotypes as predictors. Using the beads task, we also attempted to replicate the finding that reduced data-gathering is associated with delusional ideation.

STUDY RESULTS. Both delusion- and hallucination-like experiences were associated with higher precision of sensory evidence (higher drift rates) in RDM. Hallucination-like experiences were also associated with lower decision thresholds. In probabilistic reasoning, we did not find reduced data-gathering associated with any psychotic-like experiences.

CONCLUSIONS. Our findings suggest that psychotic-like experiences are associated with increased precision of sensory evidence when discriminating motion direction. A higher hallucinatory phenotype was also linked to reduced gathering of information. These specificities of information processing might represent underlying decision-making mechanisms contributing to the formation of psychotic phenomenology in the general population.

1. Introduction

Psychotic phenomenology is thought to be present along a continuum from psychotic-like experiences in healthy individuals to psychotic disorders[1–4] . The mechanisms underlying the predisposition to psychosis may be detectable at the non-clinical level along this continuum. In this study, we aimed to identify neurocomputational mechanisms associated with the emergence of the psychotic phenotype in the general population.

Predictive coding suggests that our experience of reality is constrained by neural inferences computing signals as probability distributions with their own precision[5–8]. In this view, alterations of perception or beliefs would be the result of changes in the encoding of precision (i.e., inverse of variance). For the incipient phase of psychosis, the predictive coding account of psychosis (PCA)[8] hypothesises a scenario of weak priors and/or increased precision of sensory signalling[5,6,8–10]. These neurocomputational alterations would result in a pervasive sense that reality is uncertain and inexplicable prompting individuals to undergo altered experiences of reality[11].

The hypothesis of weak prior / strong sensory evidence signals in psychosis has found support in the context of the Beads Task (BT). In BT, participants infer an unknown state of the world (e.g., the dominant colour of beads in a jar) by sequentially sampling pieces of information (e.g., coloured beads). Numerous studies using BT showed that psychosis is associated with reduced sampling of information, a phenomenon known as the jumping to-conclusion bias (JTC)[12–16]. In the BT, psychotic phenomenology has also been associated with increased influence of bottom-up information[17,18] prior belief instability[19]. This evidence from the BT suggests that the psychotic phenotype might be associated with alterations of early-stage (sensory) information processing in decision-making. If this is the case, we could expect psychotic-like experiences to be associated with increased sensory precision in perceptual decision-making.

In this study, we sought to investigate this hypothesis and extend the PCA prediction of increased sensory precision in early psychosis to the psychotic phenotype in the general population. We focused on a classic perceptual decision-making task, the Random Dot Motion task (RDM). Like BT, RDM requires participants to collect evidence from a noisy source and infer a state of the world.

Mirroring the JTC findings in BT[12–16], we expected delusional ideation to correlate negatively with sampled evidence in RDM. We applied drift-diffusion modelling (DDM) to RDM and tested whether psychotic-like experiences were associated with higher sensory precision and less accumulated evidence. We described participants' performance in terms of precision of signal detection parameterised as the drift rate (v) and quantity of accumulated evidence parameterised as the decision threshold (a). Notably, the sequential sampling model and Bayesian approaches (e.g., PCA) have been considered complementary and formally equivalent[20–23].

Preliminary to the present study, we conducted a pilot study (N=20) that showed psychotic phenotypes to be associated with lower drift rates and higher decision thresholds, contradicting the PCA predictions. Based on these data, we preregistered the present study (pre-registration link: https://osf.io/d7es8) with the hypothesis that scores of scales measuring delusional ideation, anomalous perceptions and aberrant salience would be associated with lower drift rates and higher decision thresholds. As we shall show, results were more in alignment with theoretical predictions based on PCA than our pilot data.

2. Methods

Participants

We used Amazon's Mechanical Turk service to invite a subsample of 200 participants from a larger cohort (N=1002) recruited by Sulik et al. (2023) to take part in our online study. We limited our invitations only to participants who successfully answered at least two of three attention checks in Sulik et al. (2023). The data from the draws to decision and graded estimates versions of BT (details below) and the Peters et al. Delusion Inventory (PDI)[24], a measure of delusion-like experiences, were collected by Sulik et al. (2023)[25]. In the present study, participants performed the RDM and completed the Cardiff Anomalous Perception Scale (CAPS)[26] and the Aberrant Salience Inventory (ASI)[27], respectively measuring hallucination-like experiences and life attitudes related to aberrant salience. RDM, CAPS and ASI were designed and submitted through the *Gorilla* platform and undertaken on participants' computers/laptops. Our study was approved by the ethics committee of Royal

Holloway, University of London. After a complete description of the study, the participants could ask additional questions via email and choose to take part in the study with their informed consent.

Three participants did not complete the whole experiment and six participants were excluded from the analysis because of partially missing data from their RDM performance. Statistical analyses were hence performed on 191 participants (females=87, males=104; age: M=32.2 yrs, SD=9.8).

Measures of psychotic phenotypes

We used three measures of subclinical symptoms: the 21-item PDI[24], measuring delusion-like experiences; the CAPS[26], measuring hallucination-like experiences; and the ASI[27], measuring experiences and life attitudes related to aberrant salience[28]. For each measure, we used the total score (sum of subscales). For the between-groups Bayesian hypothesis testing, participants were categorised into two groups for each measure of psychotic phenotypes using the median as a cut-off value; each participant was categorised in three ways: high- or low-PDI group, high- or low-CAPS group and high- or low-ASI group.

Random Dot Motion Task (RDM)

The visual stimuli for RDM were created through the open-access Java script made available on *Codepen.io* by Rajananda et al. (2018)[29]. On a black background, we presented a cloud composed of 500 white dots, each with a 3-pixel radius. The dots moved at 1 pixel/frame in a circular aperture with a 600-pixel diameter. The coherency of the display was manipulated by designating “noise” dots moving in randomly assigned directions, and “signal” (coherent) dots moving in one direction which was either left or right. An infinite lifetime was given to the dots, which means that each dot was redrawn only after reaching the aperture edges. At each new video frame, the dots were randomly designated to be “signal” or “noise” dots, making it impossible for the participant to infer the coherent motion by following a single dot.

Trials of two different motion-coherence conditions were presented in random order: 15 trials of high motion-coherence with 25% coherently moving dots; and 15 trials of low motion-coherence with 15% coherently moving dots. On each trial, the coherent motion was randomly assigned to be left or right. Participants were

instructed to place their index fingers ready on the "F" and "J" buttons and to express their preference about the direction by depressing the "F" button for left and the "J" button for right. Participants were prompted to answer as quickly and accurately as possible. After each trial, a green tick was displayed for correct answers and a red cross for incorrect. Fast and slow outliers were handled using the cut-off method: trials with reaction times (RT) of <200 msec or >6000 msec were excluded[30].

"Draws to decision" Beads Task (DTD-BT)

In DTD-BT, participants could draw beads in a predetermined sequence of bead colours in a ratio of 60/40 (sequence: [1- 0- 0- 1- 1- 0- 1- 1- 1- 0- 1- 1- 1- 1- 0- 0- 1- 0- 0- 1]). Participants could decide when to stop sampling and choose the jar the sequence was being drawn from. If participants wanted to draw more beads than those in the predetermined sequence, more draws were randomly generated (up to a maximum of 30), maintaining the same 60/40 colour ratio. We evaluate performance using the Draws To Decision scores (DTD), namely the number of beads the participant needed to decide which jar the beads were drawn from. Participants also gave confidence reports at three stages of DTD-BT: at 0 draws (Conf-0), after the first draw (Conf-1) and after the final draw (Conf-N when they decided to stop data-gathering).

"Graded-estimate" Beads Task (GE-BT)

In GE-BT, participants were shown a predetermined sequence of 10 beads (ratio: 60/40; sequence: [1, 1, 0, 1, 1, 0, 1, 1, 0, 1]). Instead of deciding when to stop, they were asked to estimate (from 0% to 100%) at each draw the likelihood that the sequence was being drawn from the jar of the majority colour of the sequence. Here, we computed belief adjustment (ADJ) by taking participants' probability estimates from the disconfirmatory draws. These draws (the 3rd, 6th and 9th of each sequence) were disconfirmatory in the sense that they were of a different colour than the majority of preceding draws. From the probability estimates provided in response to these draws, we subtracted the estimates provided in their preceding draws (the 2nd, 5th and 8th of each sequence) and then summed these subtractions per sequence to produce the variable ADJ. If the estimate for the majority colour was lower in the disconfirmatory draw (e.g., 50% on the 3rd) compared to the preceding one (e.g., 70%

on the 2nd) the result of the subtraction would be a negative value (e.g., 50-70 = -20) and that would indicate a decrease in belief in that possible majority colour. If the estimate for the majority colour was higher in the disconfirmatory draw compared to the preceding one, we would have a positive value of the subtraction which would stand for an increase in belief in the majority colour. So, when our total ADJ score (the overall sum of the subtractions) is negative, it indicates an overall adjustment towards disconfirmatory evidence; if positive an adjustment towards the majority colour. Because we discovered later that estimates in response to individual draws were not available from the previous data collected using this paradigm, we diverged from our pre-registered analysis and took as a dependent variable these total ADJ scores instead of estimates at each draw.

Data analysis and computational modelling

Following the data analysis plan we pre-registered, we performed three Ordinary Least Square (OLS) regression models with PDI, CAPS and ASI scores each set as the predictor of an OLS model. The dependent variables for RDM were RT and proportion correct responses for high motion-coherence, for low motion-coherence and averaged over high motion-coherence and low motion-coherence. The dependent variables for BT were DTD and total ADJ scores. However, the distributions of residuals lacked constant variance (evaluated through visual inspections of the residuals plotted against predicted values), potentially biasing the standard-error estimations of the regression models. For this reason, we additionally performed quantile (median) regression models to confirm the results from the pre-registered OLS models. We report in the main *Results* section the results from the quantile regression models, while results from the OLS models can be found in *Supplementary Materials*.

These statistical analyses were performed in an *Anaconda Python 3.6* environment using the *statsmodels 12.2* toolbox (https://www.statsmodels.org/dev/index.html). Using the *Tableone*[31] package for Python, we evaluated between-groups differences in distributions of demographic and psychometric variables. We applied the hierarchical DDM (HDDM) to RDM performance using the *HDDM 0.8.0* toolbox[32] (http://ski.clps.brown.edu/hddm_docs/index.html) in an *Anaconda Python 3.6*

environment. HDDM uses hierarchical Bayesian inference to estimate the posterior distributions of DDM parameters for each participant, allowing them to vary according to condition, group or defined linear regression models. The DDM[32,33] simulates a stochastic sampling process accumulating evidence in favour of two choices over time. The two choices are represented by two boundaries and the distance between them is quantified by the decision threshold parameter *a*, which gives a measure of how much evidence is needed to reach a decision boundary. The starting point of the sampling is represented by a parameter *z*, which we set at 0, simulating unbiased decisions. In DDM, evidence is accumulated by randomly extracting values from the distributions of the information sources[33]. The precision (or inverse variance) of the distributions determines the drift rate parameter *v*, i.e. the slope of the evidence accumulation process, which we take here as a proxy for sensory evidence precision. The more precise the extraction of information, the higher the drift rate. In all the models we performed, the two choices were coded as correct or incorrect answers (the correct answer being left or right depending on the trial), hence *v* can also be considered as an indicator of the RT-accuracy trade-off. Bitzer et al. (2014)[22] showed that when Bayesian updating is construed as the decision component of a two-alternative forced choice, it is equivalent to a DDM. They demonstrated that the drift rate parameter is equivalent to the mean value of the evidence given as input to a Bayesian updating model, approximating the precision of sensory evidence in a predictive coding framework.

We analysed the effects of psychotic phenotypes on DDM parameters using two approaches: a between-groups approach and a regression model approach, both using Bayesian statistics. For the between-groups approach, we devised HDDMs in which *v* and *a* parameters could vary between conditions and groups (see *Table 1* for details). We report here HDDMs in which we estimated parameters varying for psychotic phenotypes and motion-coherence conditions within the same models instead of those proposed in the pre-registration where low and high coherence trials were inputted to separate models (see pre-registration). The preregistered models were evaluating psychotic phenotype variability in trials of only one motion-coherence condition and could not account for within-participant variability between motion-coherence conditions, compromising the precision of parameter estimations. For these reasons, we specified HDDMs with both psychotic phenotypes

and motion-coherence conditions; specifically, we report in the *Results* section the models named (in *Table 1*) HDDM-C-PDI, HDDM-C-CAPS, HDDM-C-ASI instead of those named EC-HDDM 1, 2, 3 and HC-HDDM 1, 2, 3 (these latter models showed results consistent to those from the models presented here, see *Supplementary Materials* for further details).

Table 1. HDDM specifications. Conditions/groups according to which drift rate and decision threshold parameters were free to vary.

HC=High coherence
LC=Low coherence
LR=Linear Regression

Between-group Models	**Condition/ Groups**	**Regression Models**	**Predictors**
Null-model	None	**Null-model**	None
HDDM-C	HC vs. LC	**HDDM-LR-C**	HC vs. LC
HDDM-C-PDI	HC vs. LC | Low-PDI vs. High-PDI	**HDDM-LR-C-PDI**	PDI | HC vs. LC
HDDM-C-CAPS	HC vs. LC | Low-CAPS vs. High-CAPS	**HDDM-LR-C-CAPS**	CAPS | HC vs. LC
HDDM-C-ASI	HC vs. LC | Low-ASI vs. High-ASI	HDDM-LR-C-ASI	ASU | HC vs. LC

For the regression model approach, we used the *HDDMregressor* class of the HDDM package to run DDMs in which *v* and *a* parameters varied according to a Bayesian linear regression model specified in *Table 1*. We z-scored the values of all predictors that varied between subjects (i.e., subclinical psychotic symptom variables) and not between trials (i.e., the motion-coherence conditions) before running the models with *HDDMregressor*.

For the between-group/ -condition models, we compared posterior probability parameter distributions between conditions and groups, computing the probability that a parameter is higher or lower in one condition/group than in the other. For the Bayesian regressions, we evaluated whether the probability *P* of the posterior

probability distribution of the regression coefficient β was significantly different from 0, meaning that at least 95% of the distribution was either >0 (positive β) or <0 (negative β)[32]. To maintain a notation familiar to users of the conventional frequentist approach, we considered our results "statistically significant" when the probability of the disconfirming hypothesis was <0.05[32].

We evaluated model fit using the Deviance Information Criterion (DIC). Since DIC penalises models for complexity, lower DIC values indicate better model fit. We compared the DIC of models taking into account subclinical psychosis measures to a model where parameters did not vary according to any variable (*Null-model*) and to models taking into account only motion-coherence conditions for RDM (*HDDM-C*, *HDDM-LR-C*). In comparing the models, we considered significant a difference (Δ) of 10 DIC points[34]. We further evaluated the reliability of the winning models by simulating data and recovering parameters. Results of data simulation and parameter recovery can be found in *Supplementary Materials*.

For each DDM, Markov chain Monte Carlo simulations were used to generate 20,000 samples. The first 2,000 samples were discarded as burn-in, a thinning factor of 5 was used and outliers were set at 10%. The convergence of Markov chains was assessed by visual inspection and by computing the Gelman-Rubin statistic and verifying values ranging between 0.9 and 1.1.

3. Results

RDM RTs and accuracy

The quantile regressions (*Figure 1*) revealed positive effects of PDI and CAPS on RT mainly for high motion-coherence.

Fig. 1 Quantile regression models. Results from quantile (median) regression models with PDI, CAPS orASI as the predictor. Vertical dashes indicate the estimates for *β*. Coloured points indicate the upper and lower bounds.

HC=High motion-coherence	Conf-0= Confidence at 0 draws	*p<0.05
LC=Low motion-coherence	Conf-1= Confidence at the first draw	**p<0.01
RT=Reaction time	Conf-N= Confidence at the last draw	
DTD=Draws to decision	ADJ = Belief adjustment	

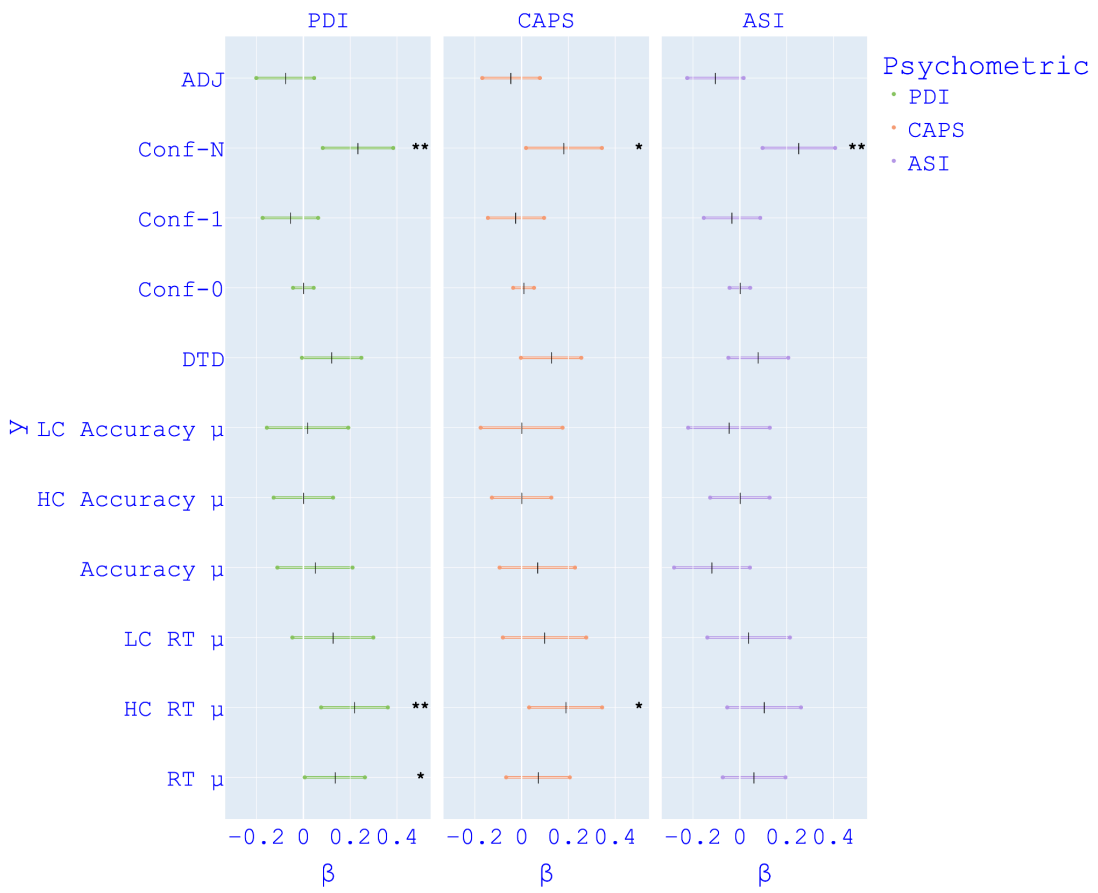

HDDM modelling: Effects on drift rate and decision threshold

Convergence. All models showed evidence of convergence from visual inspection and the Gelman-Rubin diagnostic, the values of which ranged between 0.9 and 1.

Between-group analysis. As shown in *Table 2,* models where parameters vary for both motion-coherence conditions and psychotic phenotype groups (*HDDM-PDI-C*, *HDDM-CAPS-C,HDDM-ASI-C*) showed significantly lower DIC when compared with the *Null-model* or the *HDDM-C*. In the following, therefore, we report the between-group differences in posterior probability estimates from *HDDM-PDI-C*, *HDDM-CAPS-C* and *HDDM-ASI-C.*

Table 2. ***DIC between-group HDDMs***. Values of Deviance Information Criterion (DIC) for each model in descending order (lower DIC, better fit); differences in DIC (Δ DIC) between each model and the Null-model (parameters not varying for any variable); Δ DIC between each model and the C-model (parameters varying for motion-coherence only).

	DIC	Δ DIC Null-model	Δ DIC HDDM-C
HDDM-CAPS-C	17329.78	-219.82	-135.54
HDDM-ASI-C	17345.5	-204.09	-118.82
HDDM-PDI-C	17349.19	-200.41	-115.13
HDDM-C	17464.32	-85.28	0.0
Null-model	17549.6	0.0	85.28

In all three of these models, drift rates were significantly higher in high motion-coherence than in low motion-coherence conditions (see *Fig. 2- A*), reflecting the noise in the physical stimulus (percentage of coherently moving dots), thus empirically confirming the idea that drift rate can be considered a good proxy for precision of sensory evidence[33]. Decision thresholds were lower in low motion-coherence than in high motion-coherence (see *Fig. 2-B*), showing a lower quantity of accumulated evidence for less precise stimuli.

Fig. 2 Between-group comparison. Posterior probability density distributions of drift rate (A) and decision threshold (B) for median-split groups of psychotic phenotypes. Bold lines and adjacent annotations indicate the means of the distributions.

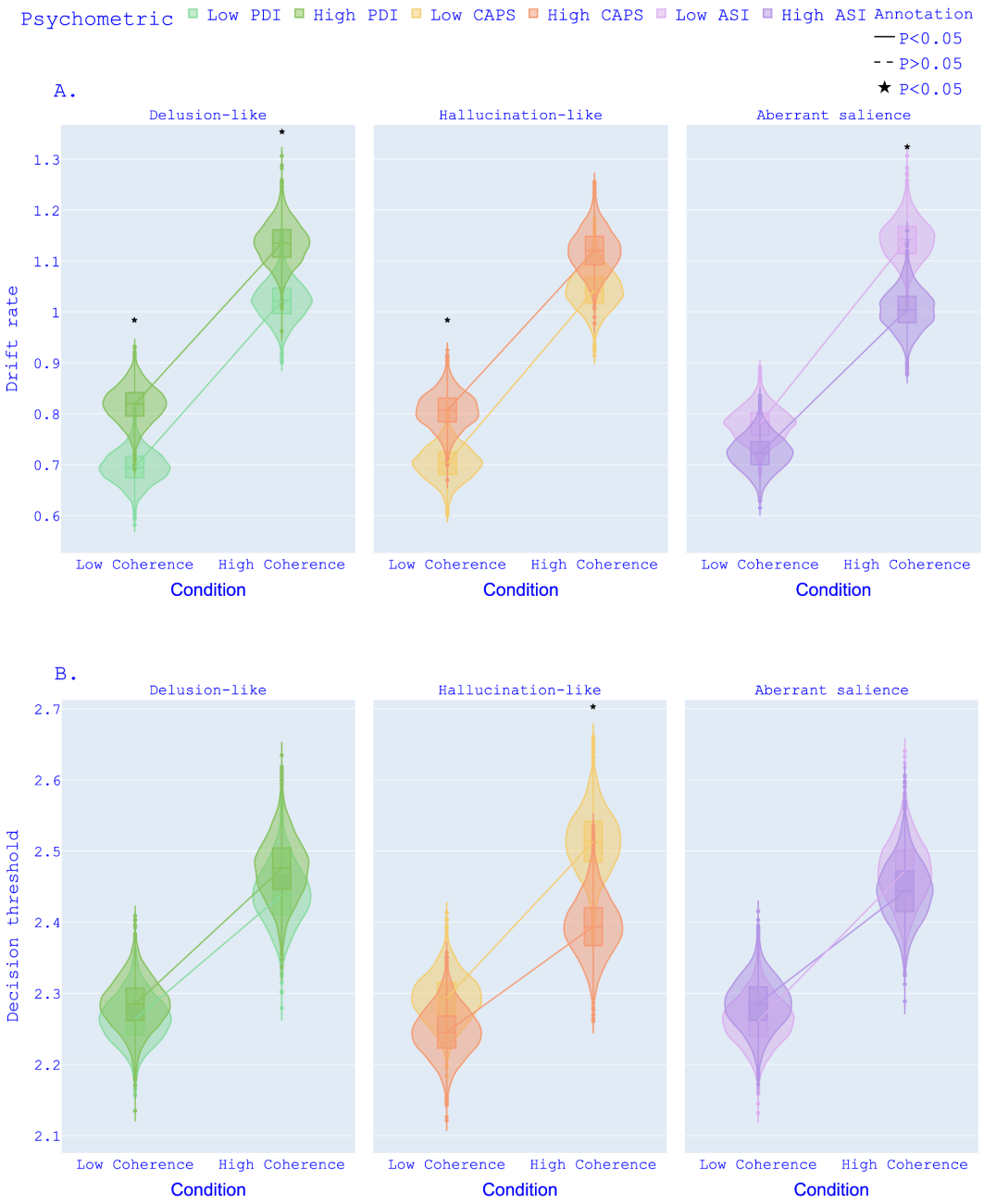

In *HDDM-PDI-C*, the high-PDI group showed significantly higher drift rates compared to the low-PDI group in both motion-coherence conditions (see *Fig. 2- A,* left). We found no difference in decision threshold between high and low PDI groups in both conditions.

In *HDDM-CAPS-C*, the high-CAPS group showed significantly higher drift rates than the low-CAPS group in low motion-coherence and trend-wise in high motion-coherence (see *Fig. 2- A,* centre). The high-CAPS group also showed a significantly lower decision threshold than the low-CAPS group in high motion-coherence but not in low motion-coherence (see *Fig. 2- B,* centre).

In *HDDM-ASI-C*, the high-ASI group showed significantly lower drift rates than the low-ASI group in high motion-coherence, but not in low motion-coherence (see *Fig. 2- A,* right). We found no significant difference in decision threshold between the high- and low-ASI groups.

***Table 3*. DIC regression HDDMs.** *Values of Deviance Information Criterion (DIC) for each model in descending order (lower DIC, better fit); differences in DIC (Δ DIC) between each model and the* Null-model (parameters not varying for any variable)*; Δ DIC between each model and the* C-model (parameters varying for motion-coherence only).

	DIC	Δ DIC Null-model	Δ DIC HDDM-C
HDDM-LR-CAPS-C	16216.39	-1333.21	-24.83
HDDM-LR-PDI-C	16229.03	-1320.57	-12.19
HDDM-LR-C	16241.22	-1308.38	0.0
HDDM-LR-ASI-C	16299.22	-1300.2758	7.63
Null-model	17549.6	0.0	1308.38

Bayesian regression analysis. Models where either PDI or CAPS were predictors with motion-coherence (*HDDM-LR-PDI-C*, *HDDM-LR-CAPS-C*) showed significantly better (i.e., lower) DICs compared to the *Null-model* and *HDDM-LR-C,* which included coherence as the only predictor. In contrast, *HDDM-LR-ASI-C* did not outperform the *HDDM-LR-C (Δ DIC=* 7.63*)*.

In *Figure 3*, we show the posterior distributions of *β* coefficients for PDI, CAPS and ASI from the models that showed the lowest DIC with these predictors (*HDDM-LR-PDI-C*, *HDDM-LR-CAPS-C* and *HDDM-LR-ASI-C*). The regression model analysis confirmed the results from the between-group analysis for PDI and CAPS; for ASI, results of the linear regression model did not align with the results from the between-group analysis and showed no effect of ASI on HDDM parameters.

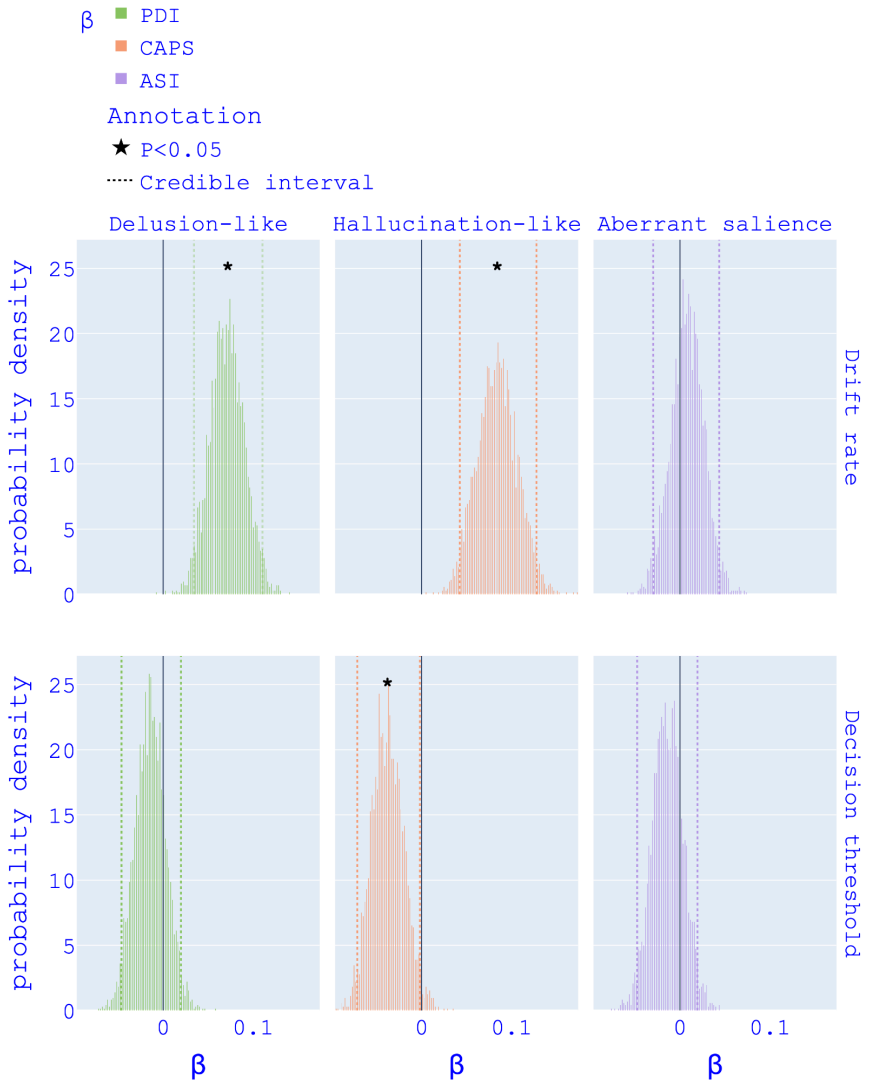

Fig. 3 HDDM regressions. Posterior probability density distributions of *β* coefficients for PDI, CAPS and ASI respectively from HDDM-LR 4, HDDM-LR 5 and HDDM-LR 6.

Probabilistic reasoning: BT

Although we found no relationship between psychotic phenotypes and DTD or ADJ (see *Fig. 1*), the results from the quantile regressions showed a positive effect of PDI, CAPS and ASI on Conf-N (i.e., confidence rating at final draw, see *Fig. 1)*.

Demographics and Subclinical psychosis

In *Table 4*, we report the main demographics of our participant sample and the means and quartiles of the distributions for high and low PDI, CAPS, and ASI groups. Only between low-CAPS and high-CAPS groups was there a significant difference in age with participants in the high-CAPS group being older (t (189) = -0.36, p<0.05). In all group pairs, we see an uneven distribution of the psychotic phenotype measures: CAPS and ASI scores are higher for the high-PDI group, PDI and ASI scores are higher for the high-CAPS group, PDI and CAPS scores are higher for the high-ASI group.

Table 4. Differences between psychotic phenotype groups. *Median values of demographic, psychometric and psychotic trait variables with tests of their group differences (significant differences in bold).*

		Overall	*High-PDI*	*Low-PDI*	*p value*	*High-CAPS*	*Low-CAPS*	*p*	*High-ASI*	*Low-ASI*	*p value*
	N	191	95	96		96	95		90	101	
Age, mean (SD)		36.1 (9.9)	36.5 (9.2)	35.6 (10.5)	0.56*	37.8 (10.3)	34.3 (9.1)	**<0.05***	36.6 (10.2)	35.6 (9.6)	0.499*
Gender, n (%)	***F***	87 (45.5)	42 (43.3)	45 (47.9)	0.625†	47 (49.0)	40 (42.1)	0.42†	38 (42.2)	49 (48.5)	0.468†
	M	104 (54.5)	55 (56.7)	49 (52.1)		49 (51.0)	55 (57.9)		52 (57.8)	52 (51.5)	
PDI, median [Q1,Q3]		22.0 [6.0,43.0]	43.0 [31.0,60.0]	6.0 [0.0,14.8]	**<0.001°**	36.5 [18.5,58.0]	10.0 [0.0,27.0]	**<0.001°**	35.0 [19.2,58.0]	13.0 [0.0,27.0]	**<0.001°**
CAPS, median [Q1,Q3]		13.0 [0.0,37.5]	30.0 [8.0,56.0]	6.0 [0.0,18.0]	**<0.001°**	37.5 [25.0,59.0]	0.0 [0.0,6.5]	**<0.001°**	32.5 [17.2,59.0]	0.0 [0.0,11.0]	**<0.001°**
ASI, median [Q1,Q3]		6.0 [2.0,12.0]	9.0 [6.0,15.0]	3.0 [1.0,7.0]	**<0.001°**	10.0 [6.8,16.0]	2.0 [0.0,5.5]	**<0.001°**	13.0 [9.0,17.0]	2.0 [0.0,4.0]	**<0.001°**
CRT, median [Q1,Q3]		0.7 [0.4,0.9]	0.7 [0.4,0.9]	0.7 [0.3,0.9]	0.525°	0.7 [0.3,0.9]	0.7 [0.4,0.9]	0.848°	0.7 [0.4,0.9]	0.7 [0.3,0.9]	0.679°

*Two Sample T-test**
Chi-squared†
Kruskal-Wallis°

Q1=25th percentile
Q3= 75th percentile
SD=Standard Deviation
p=p-value

4. Discussion

Taking the drift rate as a proxy for precision of sensory evidence[20–23], and decision threshold as a quantification of accumulated evidence, we tested in a classic RDM task if and how these DDM parameters varied with measures of psychotic phenotype.

In our non-clinical sample, both hallucination-like and delusion-like experiences were associated with higher precision of sensory evidence in RDM (i.e., drift rate), while only hallucination-like experiences predicted lower decision thresholds.

We also attempted to replicate previous studies showing reduced sampling (e.g., fewer samples of evidence) in probabilistic reasoning, namely in the BT, associated with delusional ideation. After controlling for performance attentiveness, we reproduced Sulik et al's (2023)[25] results in our subsample where we found no evidence of reduced sampling in probabilistic reasoning for participants higher in delusional ideation. This suggests that in subclinical psychosis, alterations in inferential processes attributable to sensory precision might be more prominent and detectable in the perceptual rather than in the cognitive domain.

Psychotic-like Experiences and Perceptual Inference

We showed that hallucination-like (i.e., CAPS) and delusion-like (i.e., PDI) experiences are associated with higher precision of sensory evidence (i.e. drift rate) in perceptual inference, suggesting a link between perceptual mechanisms and the formation of anomalous perceptions and beliefs. Alterations of perceptual information processing could precede and potentially contribute to anomalous perceptions as well as to changes in the belief system. This supports the idea in the PCA that the psychotic phenotype might be driven by the urgency of explaining persistent prediction error signals[5,8,9,11]. In this view, in a prodromal phase, an overly precise perceptual encoding of otherwise irrelevant stimuli would undermine the stability of prior beliefs, producing a pervasive sense of inexplicability.

Previous studies have associated psychotic-like experiences with increased influence of prior beliefs[35–38]. These studies involved the discrimination of visual stimuli, including living beings and human faces, in static noisy pictures. This evidence seems to suggest that the psychotic phenotype is associated with strong perceptual priors when discriminating static socially meaningful stimuli[35–38]. Our findings support the idea that in a different perceptual context, that is when discriminating motion of socially neutral stimuli, the psychotic phenotype is characterised by increased precision of sensory evidence. We did not induce in our participants any prior knowledge of the direction of coherent moving dots, so we have not measured the impact of priors on our paradigm. However, our results can be

complemented by evidence from Stuke et al. (2018)[39], who found an association of PDI with weaker perceptual priors in the RDM. Together, ours and Stuke et al.'s study suggest that discrimination of motion signals in the psychotic phenotype is characterised by weaker prior influence and increased precision of sensory evidence. Future studies could aim to investigate within the same sample how the nature of perceptual stimuli (socially meaningful vs. neutral; static vs. in-motion discrimination) impacts neurocomputational specificities associated with the psychotic phenotype.

Differently from PDI and CAPS, aberrant salience as measured by ASI was associated with lower (rather than higher) precision of sensory evidence and lower decision thresholds in the between-group analysis. Like PDI and CAPS, ASI is also considered to measure a psychotic trait[27] and in our study, all three measures were positively associated with each other (see *Table 2*). This discrepancy in the impact on RDM performance between ASI and other subclinical traits might represent a dissociation between core psychotic-like symptoms (delusional ideation and anomalous perceptions) and aberrant salience of stimuli. However, when ASI is taken as a continuous variable, the regression model did not show any effect of ASI and did not outperform the model taking only motion-coherence conditions into account. Thus, results on ASI appear to be less robust than those we obtained for PDI and CAPS, which were reproduced in both analysis versions: group and regression.

Psychotic-like Experiences and Cognitive Inference

The DTD-BT is a probabilistic reasoning task in which delusion-prone and delusional participants in previous studies showed reduced evidence sampling, a phenomenon known as JTC[12–16]. It remains uncertain if this behavioural pattern is specifically associated with delusional symptomatology. Different studies have pointed out how other factors modulate sampling in BT and possibly create an illusory positive association between JTC and delusions: miscomprehension of the task[40], motivation[41], socio-economic status[42] or general cognitive ability[43]. Ross et al. (2016)[44] found that PDI had no effect on DTD, and showed that cognitive style (analytical vs. intuitive) could be considered a more reliable predictor of sampling behaviour in BT. Sulik et al. (2023) confirmed this view and although in an analysis of their full sample, they found a negative relationship between PDI and DTD, the

exclusion of low-quality data (i.e., participants who did not pass attention checks during the task) ruled out any effect of PDI on DTD. When we analysed data from a subsample of attentive participants of Sulik et al. 's cohort, we also did not find any JTC in relation to delusion-like experiences (reproducing Sulik et al.'s resutls in our subsample) or to other subclinical psychosis measures. These results illustrate the sporadic nature of the association between delusion-like beliefs and reduced sampling in the BT[13] and show how alterations of perceptual inference (e.g., on the RDM task) might represent instead a more prominent feature of subclinical psychosis.

We did not find any significant relationship between psychotic-like experiences and ADJ. Although this BT behavioural pattern has been shown in schizophrenia patients with delusions[17,19,45], it has repeatedly failed to be replicated in individuals from the general population with high scores for delusional ideation [25,40,46]. Our study therefore supports the idea that ADJ does not vary with measures of subclinical psychosis.

Neurofunctional Implications

We identified a computational pattern in RDM task performance, namely increased precision of sensory evidence, that varies along with psychotic phenotypes. Given that RDM is a well-studied paradigm in animal and human neurophysiology, we would like to suggest here some hypotheses about possible neural mechanisms underpinning our findings. In RDM, neural firing-rates in the lateral intraparietal cortex (LIP) of monkeys[47–49] and the central parietal positivity (CPP) in humans [50,51] show a similar pattern: they ramp up during evidence accrual until they reach a peak and dampen after the decision is taken. Behaving as a drift rate, the slope of the build-up of LIP firing rates as well as the amplitude of CPP are higher when the precision on the evidence is higher (e.g., higher motion-coherence in RDM). Moreover, this same centro-parietal ramping activity seems to track not merely the noise of the physical stimuli (e.g. motion-coherence), but to reflect the subjective precision ascribed to the sensory signal (participant's confidence)[52–54]. Interestingly, the slope of cumulative activity of neurons in posterior parietal cortex (PPC) recorded with magneto-encephalography during RDM correlates with the synaptic gain of superficial pyramidal cells as simulated through dynamic causal modelling[21], suggesting the hypothesis that PPC superficial cells encode the precision ascribed to

sampled evidence. We can hence speculate that altered synaptic gain in PPC superficial pyramidal cells may underpin the information processing specificities we found associated with subclinical psychosis. Acknowledging the association between psychotic-like experiences and higher drift rates in RDM shown here, future studies might aim at describing any distinctive relation of drift rate with PPC activity in psychosis-prone individuals.

In summary, our study highlights an association of both hallucination- and delusion-like experiences with increased sensory precision in perceptual inference of motion of socially neutral stimuli. A higher hallucinatory phenotype was also associated with a decreased quantity of gathered information. We did not find any significant behavioural pattern in cognitive inference (i.e., on the draws to decision beads task) associated with psychotic-like experiences. More broadly, our findings suggest that alterations in precision encoding of sensory information might be implicated in psychotic phenomenology in the general population, in line with the predictions of PCA. Investigating whether and how the neurocomputational specificities we found at the subclinical level vary in the clinical population could shed light on mechanisms driving the formation of full-blown psychotic symptoms.

Acknowledgments

This work was supported by a grant from the *NOMIS Foundation* ("Collective Delusions: Social Identity and Sci- entific Misbeliefs").

References

1. Mennigen E, Bearden CE. Psychosis Risk and Development: What Do We Know From Population-Based Studies? *Biol Psychiatry*. 2020;88(4):315-325. doi:10.1016/j.biopsych.2019.12.014
2. Strauss JS. Hallucinations and Delusions as Points on Continua Function: Rating Scale Evidence. *Arch Gen Psychiatry*. 1969;21(5):581-586. doi:10.1001/archpsyc.1969.01740230069010
3. van Os J. Strauss (1969) revisited: a psychosis continuum in the general

population? *Schizophr Res*. Published online 2000.

4. van Os J, Linscott RJ, Myin-Germeys I, Delespaul P, Krabbendam L. A systematic review and meta-analysis of the psychosis continuum: evidence for a psychosis proneness–persistence–impairment model of psychotic disorder. *Psychol Med*. 2009;39(2):179-195. doi:10.1017/S0033291708003814

5. Adams RA, Stephan KE, Brown HR, Frith CD, Friston KJ. The Computational Anatomy of Psychosis. *Front Psychiatry*. 2013;4. doi:10.3389/fpsyt.2013.00047

6. Friston K, Brown HR, Siemerkus J, Stephan KE. The dysconnection hypothesis (2016). *Schizophr Res*. 2016;176(2-3):83-94. doi:10.1016/j.schres.2016.07.014

7. Friston K, Kiebel S. Predictive coding under the free-energy principle. *Philos Trans R Soc B Biol Sci*. 2009;364(1521):1211-1221. doi:10.1098/rstb.2008.0300

8. Sterzer P, Adams RA, Fletcher P, et al. The Predictive Coding Account of Psychosis. *Biol Psychiatry*. 2018;84(9):634-643. doi:10.1016/j.biopsych.2018.05.015

9. Corlett PR, Frith CD, Fletcher PC. From drugs to deprivation: a Bayesian framework for understanding models of psychosis. *Psychopharmacology (Berl)*. 2009;206(4):515-530. doi:10.1007/s00213-009-1561-0

10. Stephan KE, Friston KJ, Frith CD. Dysconnection in Schizophrenia: From Abnormal Synaptic Plasticity to Failures of Self-monitoring. *Schizophr Bull*. 2009;35(3):509-527. doi:10.1093/schbul/sbn176

11. Carhart-Harris RL, Friston KJ. REBUS and the Anarchic Brain: Toward a Unified Model of the Brain Action of Psychedelics. Barker EL, ed. *Pharmacol Rev*. 2019;71(3):316-344. doi:10.1124/pr.118.017160

12. Fine C, Gardner M, Craigie J, Gold I. Hopping, skipping or jumping to conclusions? Clarifying the role of the JTC bias in delusions. *Cognit Neuropsychiatry*. 2007;12(1):46-77. doi:10.1080/13546800600750597

13. Ross RM, McKay R, Coltheart M, Langdon R. Jumping to Conclusions About the Beads Task? A Meta-analysis of Delusional Ideation and Data-Gathering. *Schizophr Bull*. 2015;41(5):1183-1191. doi:10.1093/schbul/sbu187

14. Evans S, Averbeck B, Furl N. Jumping to conclusions in schizophrenia. *Neuropsychiatr Dis Treat*. Published online July 2015:1615. doi:10.2147/NDT.S56870

15. Dudley R, Taylor P, Wickham S, Hutton P. Psychosis, Delusions and the "Jumping to Conclusions" Reasoning Bias: A Systematic Review and Meta-analysis. *Schizophr Bull*. 2016;42(3):652-665. doi:10.1093/schbul/sbv150

16. McLean BF, Mattiske JK, Balzan RP. Association of the Jumping to Conclusions and Evidence Integration Biases With Delusions in Psychosis: A Detailed Meta-analysis. *Schizophr Bull*. 2017;43(2):344-354. doi:10.1093/schbul/sbw056

17. Jardri R, Duverne S, Litvinova AS, Denève S. Experimental evidence for circular inference in schizophrenia. *Nat Commun*. 2017;8(1):14218.

doi:10.1038/ncomms14218

18. Stuke H, Stuke H, Weilnhammer VA, Schmack K. Psychotic Experiences and Overhasty Inferences Are Related to Maladaptive Learning. Einhäuser W, ed. *PLOS Comput Biol*. 2017;13(1):e1005328. doi:10.1371/journal.pcbi.1005328

19. Adams RA, Napier G, Roiser JP, Mathys C, Gilleen J. Attractor-like Dynamics in Belief Updating in Schizophrenia. *J Neurosci*. 2018;38(44):9471-9485. doi:10.1523/JNEUROSCI.3163-17.2018

20. Hesselmann G, Sadaghiani S, Friston KJ, Kleinschmidt A. Predictive Coding or Evidence Accumulation? False Inference and Neuronal Fluctuations. *PLOS ONE*. 2010;5(3):e9926. doi:10.1371/journal.pone.0009926

21. FitzGerald THB, Moran RJ, Friston KJ, Dolan RJ. Precision and neuronal dynamics in the human posterior parietal cortex during evidence accumulation. *NeuroImage*. 2015;107:219-228. doi:10.1016/j.neuroimage.2014.12.015

22. Bitzer S, Park H, Blankenburg F, Kiebel S. Perceptual decision making: drift-diffusion model is equivalent to a Bayesian model. *Front Hum Neurosci*. 2014;8. Accessed October 9, 2022. https://www.frontiersin.org/articles/10.3389/fnhum.2014.00102

23. Fard PR, Park H, Warkentin A, Kiebel SJ, Bitzer S. A Bayesian Reformulation of the Extended Drift-Diffusion Model in Perceptual Decision Making. *Front Comput Neurosci*. 2017;11. Accessed September 2, 2023. https://www.frontiersin.org/articles/10.3389/fncom.2017.00029

24. Peters E, Joseph S, Day S, Garety P. Measuring Delusional Ideation: The 21-Item Peters et al. Delusions Inventory (PDI). *Schizophr Bull*. 2004;30(4):1005-1022. doi:10.1093/oxfordjournals.schbul.a007116

25. Sulik J, Ross RM, Balzan R, McKay R. Delusion-like beliefs and data quality: Are classic cognitive biases artifacts of carelessness? *J Psychopathol Clin Sci*. 2023;132(6):749-760. doi:10.1037/abn0000844

26. Bell V, Halligan PW, Ellis HD. The Cardiff Anomalous Perceptions Scale (CAPS): A New Validated Measure of Anomalous Perceptual Experience. *Schizophr Bull*. 2006;32(2):366-377. doi:10.1093/schbul/sbj014

27. Cicero DC, Kerns JG, McCarthy DM. The Aberrant Salience Inventory: A new measure of psychosis proneness. *Psychol Assess*. 2010;22(3):688-701. doi:10.1037/a0019913

28. Kapur S. Psychosis as a State of Aberrant Salience: A Framework Linking Biology, Phenomenology, and Pharmacology in Schizophrenia. *Am J Psychiatry*. 2003;160(1):13-23. doi:10.1176/appi.ajp.160.1.13

29. Rajananda S, Lau H, Odegaard B. A Random-Dot Kinematogram for Web-Based Vision Research. *J Open Res Softw*. 2018;6:6. doi:10.5334/jors.194

30. Voss A, Nagler M, Lerche V. Diffusion models in experimental psychology: A practical introduction. *Exp Psychol*. 2013;60(6):385-402. doi:10.1027/1618-3169/a000218

31. Pollard TJ, Johnson AEW, Raffa JD, Mark RG. tableone: An open source Python package for producing summary statistics for research papers. *JAMIA Open*. 2018;1(1):26-31. doi:10.1093/jamiaopen/ooy012

32. Wiecki TV, Sofer I, Frank MJ. HDDM: Hierarchical Bayesian estimation of the Drift-Diffusion Model in Python. *Front Neuroinformatics*. 2013;7:14. doi:10.3389/fninf.2013.00014

33. Ratcliff R, Smith PL, Brown SD, McKoon G. Diffusion Decision Model: Current Issues and History. *Trends Cogn Sci*. 2016;20(4):260-281. doi:10.1016/j.tics.2016.01.007

34. Spiegelhalter DJ, Best NG, Carlin BP, Van Der Linde A. Bayesian measures of model complexity and fit. *J R Stat Soc Ser B Stat Methodol*. 2002;64(4):583-639. doi:10.1111/1467-9868.00353

35. Davies DJ, Teufel C, Fletcher PC. Anomalous Perceptions and Beliefs Are Associated With Shifts Toward Different Types of Prior Knowledge in Perceptual Inference. *Schizophr Bull*. 2018;44(6):1245-1253. doi:10.1093/schbul/sbx177

36. Furl N, McKay R, Coltheart M. The Paradox of Delusions: Are Deluded Individuals Resistant to Evidence? Published online January 29, 2022. doi:10.31234/osf.io/e37c2

37. Teufel C, Subramaniam N, Dobler V, et al. Shift toward prior knowledge confers a perceptual advantage in early psychosis and psychosis-prone healthy individuals. *Proc Natl Acad Sci*. 2015;112(43):13401-13406. doi:10.1073/pnas.1503916112

38. Stuke H, Kress E, Weilnhammer VA, Sterzer P, Schmack K. Overly Strong Priors for Socially Meaningful Visual Signals Are Linked to Psychosis Proneness in Healthy Individuals. *Front Psychol*. 2021;12. Accessed March 26, 2023. https://www.frontiersin.org/articles/10.3389/fpsyg.2021.583637

39. Stuke H, Weilnhammer VA, Sterzer P, Schmack K. Delusion Proneness is Linked to a Reduced Usage of Prior Beliefs in Perceptual Decisions. *Schizophr Bull*. Published online January 20, 2018. doi:10.1093/schbul/sbx189

40. Balzan R, Delfabbro P, Galletly C. Delusion‐proneness or miscomprehension? A re‐examination of the jumping‐to‐conclusions bias. *Aust J Psychol*. 2012;64(2):100-107. doi:10.1111/j.1742-9536.2011.00032.x

41. McKay R, Langdon R, Coltheart M. Need for Closure, Jumping to Conclusions, and Decisiveness in Delusion-Prone Individuals. *J Nerv Ment Dis*. 2006;194(6):422. doi:10.1097/01.nmd.0000221353.44132.25

42. Baker SC, Konova AB, Daw ND, Horga G. A distinct inferential mechanism for delusions in schizophrenia. *Brain*. 2019;142(6):1797-1812. doi:10.1093/brain/awz051

43. Tripoli G, Quattrone D, Ferraro L, et al. Jumping to conclusions, general intelligence, and psychosis liability: findings from the multi-centre EU-GEI case-control study. *Psychol Med*. 2021;51(4):623-633.

doi:10.1017/S003329171900357X

44. Ross RM, Pennycook G, McKay R, Gervais WM, Langdon R, Coltheart M. Analytic cognitive style, not delusional ideation, predicts data gathering in a large beads task study. *Cognit Neuropsychiatry*. 2016;21(4):300-314. doi:10.1080/13546805.2016.1192025

45. Langdon R, Ward PB, Coltheart M. Reasoning Anomalies Associated With Delusions in Schizophrenia. *Schizophr Bull*. 2010;36(2):321-330. doi:10.1093/schbul/sbn069

46. Colbert SM, Peters ER. NEED FOR CLOSURE AND JUMPING-TO-CONCLUSIONS IN DELUSION-PRONE INDIVIDUALS. *J Nerv Ment Dis*. 2002;190(1):27.

47. Shadlen MN, Newsome WT. Motion perception: seeing and deciding. *Proc Natl Acad Sci*. 1996;93(2):628-633. doi:10.1073/pnas.93.2.628

48. Roitman JD, Shadlen MN. Response of Neurons in the Lateral Intraparietal Area during a Combined Visual Discrimination Reaction Time Task. *J Neurosci*. 2002;22(21):9475-9489. doi:10.1523/JNEUROSCI.22-21-09475.2002

49. Hanks TD, Summerfield C. Perceptual Decision Making in Rodents, Monkeys, and Humans. *Neuron*. 2017;93(1):15-31. doi:10.1016/j.neuron.2016.12.003

50. O'Connell RG, Dockree PM, Kelly SP. A supramodal accumulation-to-bound signal that determines perceptual decisions in humans. *Nat Neurosci*. 2012;15(12):1729-1735. doi:10.1038/nn.3248

51. Kelly SP, O'Connell RG. Internal and External Influences on the Rate of Sensory Evidence Accumulation in the Human Brain. *J Neurosci*. 2013;33(50):19434-19441. doi:10.1523/JNEUROSCI.3355-13.2013

52. Kiani R, Shadlen MN. Representation of Confidence Associated with a Decision by Neurons in the Parietal Cortex. *Science*. 2009;324(5928):759-764. doi:10.1126/science.1169405

53. Tagliabue CF, Veniero D, Benwell CSY, Cecere R, Savazzi S, Thut G. The EEG signature of sensory evidence accumulation during decision formation closely tracks subjective perceptual experience. *Sci Rep*. 2019;9(1):4949. doi:10.1038/s41598-019-41024-4

54. Pereira M, Megevand P, Tan MX, et al. Evidence accumulation determines conscious access. Published online July 11, 2020:2020.07.10.196659. doi:10.1101/2020.07.10.196659

Supplementary materials

1. Distributions of psychotic phenotype measures

For a full display of the psychotic phenotype data in our sample, we report here the medians and the frequency distribution in sample percentage for PDI, CAPS and ASI (Fig 1-A-B-C).

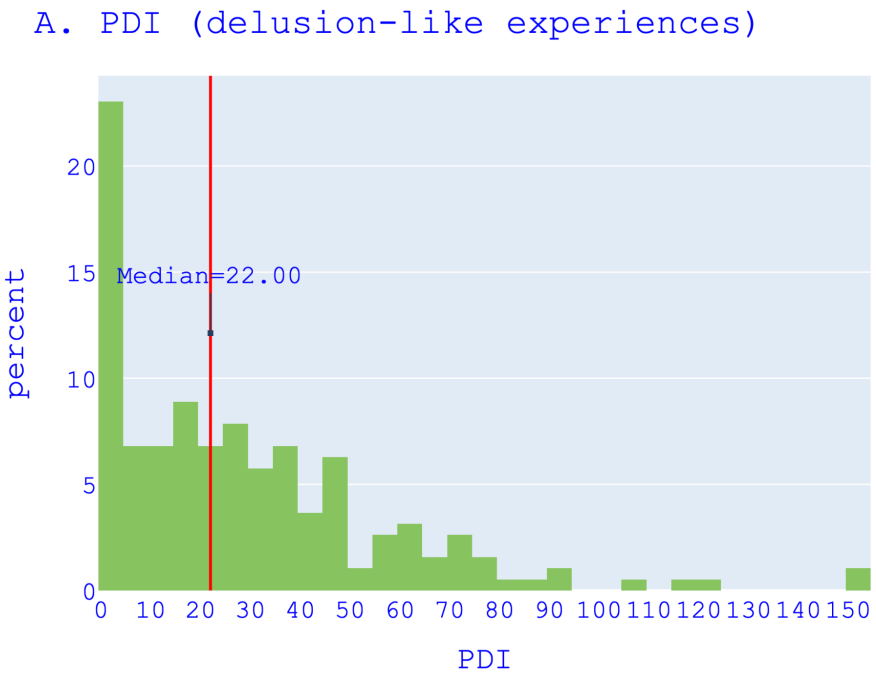

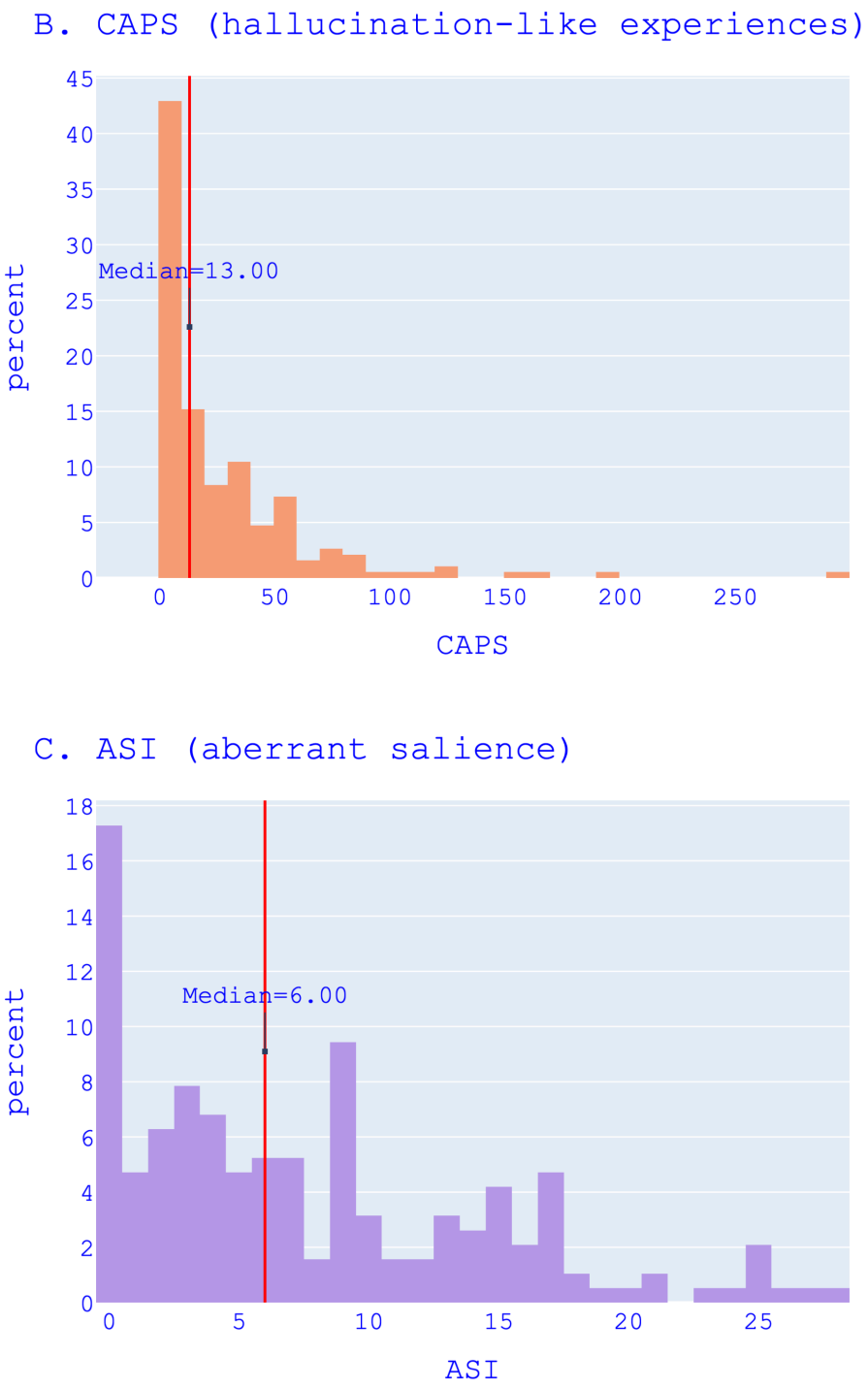

Fig 1. Frequency distribution of psychotic phenotype measures. Distribution in participant percentage of (A) Peters et al. Delusion Inventory (PDI), (B) Cardiff Anomalous Perceptions Scale (CAPS) and (C) Aberrant Salience Inventory (ASI).

2. Data Simulation and Parameter Recovery

We provide here a comprehensive overview of the performance of the hierarchical drift-diffusion models (HDDMs) fitted to the data from the Random Dot Motion task (RDM). Following good practice guidance in computational modelling of behaviour (Vandekerckhove & Tuerlinckx, 2007; Wiecki et al., 2013; Wilson & Collins, 2019), we assessed the validity of our models through two main steps: simulation of data and recovery of parameters. By evaluating the performance of our models, we also evaluated the relative merits of different modelling techniques, including median split versus regression techniques with a view to developing modelling guidance for future studies. Here, we present a qualitative comparison between observed and simulated data, followed by the recovery of the estimated parameters. In *Section 1*, we present the methodology we used, and in *Sections 2* and *3* the results of data simulation and parameter recovery. Finally, in the *Discussion* Section, we comment and draw conclusions from *Sections 2* and *3*.

2.1 Methodology

Data simulation. We simulated the data using the *hddm.generate.gen_rand_data(...)* function of the *HDDM 0.8.0* package (Wiecki et al., 2013). This function simulates reaction times (RTs) and responses given the mean and standard deviation of DDM parameters. The function allows specification of the values of parameters for different discrete levels (e.g., conditions or groups), and reproduces the size and structure of the data in terms of the number of trials and participants per level. For between-group HDDMs, we inputted the mean and standard deviation of the fitted parameters for each condition/group level and obtained RTs and responses for each group/condition.

For regression HDDMs, more steps than for the between-group HDDMs were needed to simulate data sets that reproduce the structure of the observed ones. In fact, in the regression HDDMs, we had a two-level dummy coded variable (motion-coherence) and a continuous variable (PDI, CAPS or ASI) predicting each parameter of interest (drift rate or decision threshold). One obstacle in the data simulation was to inform the simulation function of the effect of the continuous variable on the parameters. In fact, *hddm.generate.gen_rand_data(...)* simulates data given discrete parameter values. We approached this problem by computing a mean

predicted value of parameters for each level of the dummy coded variable including the regression coefficients of the continuous variable in each level as shown below in *Equation 1* and *Equation 2*.

$$(1) \qquad c = (0, 1)\,, Y = a + b_1(c) + b_2(X)$$

In *Equation 1*, *Y* denotes the vector of predicted values (e.g., drift rate) for the level of the dummy coded variable *c* ($c=0 \vee c=1$), *X* the continuous variable predictor (e.g., PDI, CAPS or ASI) and *a* the intercept. We computed *Y* for both $c=0$ and $c=1$ and obtained two vectors, one for each level of the dummy coded variable, of the predicted parameters Y_0 and Y_1. We then averaged the values for each array and obtained the average Y_0 for level 0 and average Y_1 for level 1, which are the mean predicted parameters to be inputted to *hddm.generate.gen_rand_data(...)*. To simulate the models, we needed to include in the simulated dataset a value of the continuous variable (PDI, CAPS and ASI) per simulated participant. Since the data were simulated employing a stochastic approximation of the effect of the continuous variable on the parameters (i.e., the mean predicted value), we took a similarly stochastic approach and pooled randomly from our empirical data values of PDI, CAPS and ASI and assigned them to the simulated participants.

To capture how well the models predict RTs model, we simulated 100 datasets for each model and averaged the 10th, 30th, 50th, 70th and 90th quantiles of the simulated RT distributions for correct and error responses. We then plotted in a linearity plot (or QQ plot, shown in *Figure 2* and *Figure 6*) the observed RT quantiles on the x-axis and the simulated quantiles on the y-axis to obtain a line that we contrasted with an "optimal simulation line" drawn by plotting observed quantiles on both axes. To quantify the distance between the simulated and the observed quantiles, we took as metrics the root-mean-squared error (RMSE) and the Standardised Mean Difference (SMD; also known as Cohen's D). RMSE is a measure of the average difference between predicted and observed values and it is expressed in the units of the variable value. The SMD is the ratio of the difference between the means and the sum of the standard deviations of the two distributions. Unlike the RMSE, the SMD is a standardised metric suitable for comparing the prediction performance across

different magnitudes of RTs (e.g. between correct and error responses, the latter usually slower).

Parameter recovery. We performed the parameter recovery for between-group and regression HDDMs reported in the *Results* section. In the between-group HDDMs, drift rate and decision threshold were allowed to vary for motion-coherence (high vs. low) and median-split groups for PDI (HDDM-PDI-C), CAPS (HDDM-CAPS-C), and ASI (HDDM-ASI-C). In the regression models, drift rate and decision threshold were free to vary as the response variable of a linear regression model with motion-coherence and PDI (HDDM-LR-PDI-C), CAPS (HDDM-LR-CAPS-C) or ASI (HDDM-LR-ASI-C) scores as predictors. We refer here to these models as *empirical models*, because their parameters were estimated from fits to human RTs and accuracy rather than to simulated data. For each empirical model, we simulated one dataset (following the procedures described in the preceding paragraph) and fitted an equivalent *simulation model*. We evaluated the distance between the distributions of the simulated and empirical parameters using RMSE and SMD. For between-group HDDMs, we computed RMSE and SMD between the estimated and simulated distributions of DDM parameters per group (e.g. low-PDI) or condition (e.g. high motion-coherence). For regression HDDMs, we computed the RMSE and SMD between the empirical and simulated β coefficients. Lower RMSE and SMD between estimated and simulated parameters indicate a better recovery and a more precise estimation of the true parameters for groups, conditions or predicted variables. Additionally, we considered whether the simulation models could reproduce the DDM parameter differences and β coefficients estimate reported in the results of the empirical models. If the simulated parameters adequately recover the effects observed, it suggests that the model is accurately capturing the processes that produced the empirical data.

Overall, the recovery of parameters is an essential step in validating computational models of behaviour as it helps to establish the reliability, validity, and generalizability of the model's results, and increases confidence in the model's ability to accurately describe and explain data from different samples of the same population (Vandekerckhove & Tuerlinckx, 2007; Wiecki et al., 2013; Wilson & Collins, 2019).

2.2 Data simulation and parameter recovery results

Here, we report the data simulation and parameter recovery for between-group and regression HDDMs. In *Figure 1*, we show the distribution of RTs inputted to these models.

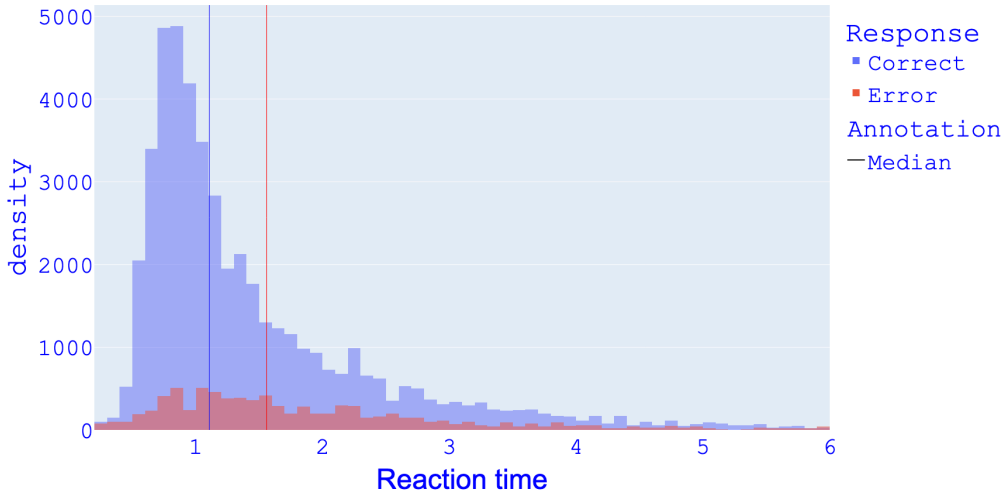

Fig. 1 RT distribution Study1. Distribution of reaction times (in seconds) for correct and error responses as inputted to HDDMs in *Study 1*; fast outliers cut-off: 0.2 s; slow outliers cut-off: 6 s.

Between-group HDDMs

In *Figure 2*, we show the quantiles of simulated RT distribution over the observed RT quantiles for between-group models. The first three quantiles of predicted RTs for correct responses align almost completely with the observed quantiles, while for the fourth and the last quantiles, RTs have been underestimated with a mean RMSE of 0.123 s. Predicted RT quintiles for error responses showed a general underestimation with a mean RMSE of 0.654 s for error responses.

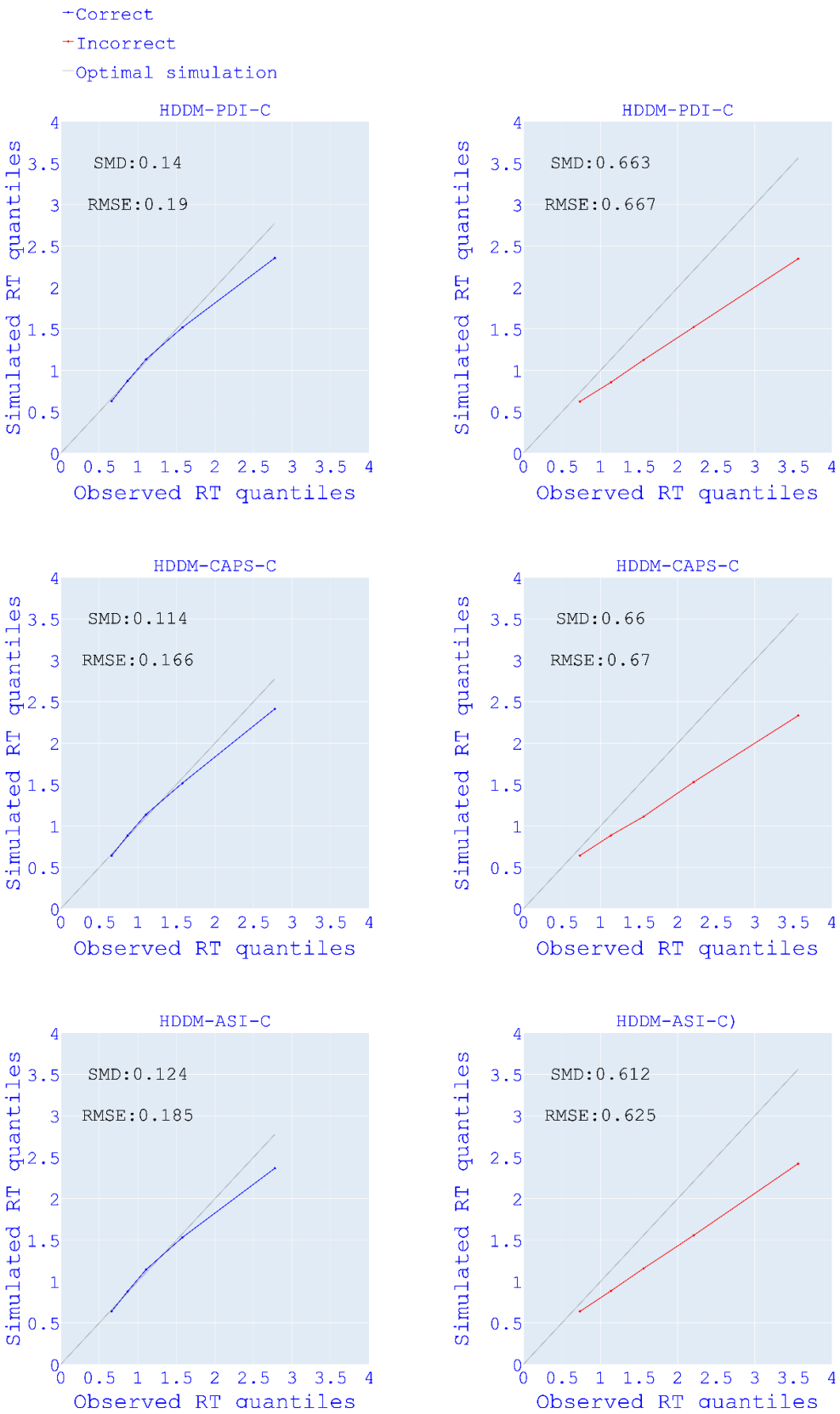

Fig.2 RT predictions of between-group HDDMs Study 1. Linearity plots of observed reaction time (RT) quantiles (x-axis) and simulated RT quantiles (y-axis) for correct and error responses of between-group models in *Study 1*. SMD= Standardised mean difference; RMSE= Root mean squared error.

From *Figure-3*, *-4* and *-5*, it can be noticed that simulated parameters tend to be higher than the estimated parameters. This overestimation did not prevent the recovery of the significant differences in drift rate between median-split groups shown by the empirical models (see: *Figure 3* top-right; *Figure 4* top-left and bottom-right; *Figure 5* top-left). The effect of PDI-grouping on the drift rate in low precision of motion-coherence was the only one not recovered in the simulation model, although the simulated pattern shows a trend in the same direction as the empirical result; see *Figure-5* top-right). Another divergence between empirical and simulation models is evident in decision threshold estimates for the high-PDI group in high precision (SMD=-5.57, RMSE=0.226); see *Figure-5* bottom-right), where the simulation model shows a significant difference between low- and high-PDI groups that is not present in the estimates of the empirical model which show only a trend in this direction.

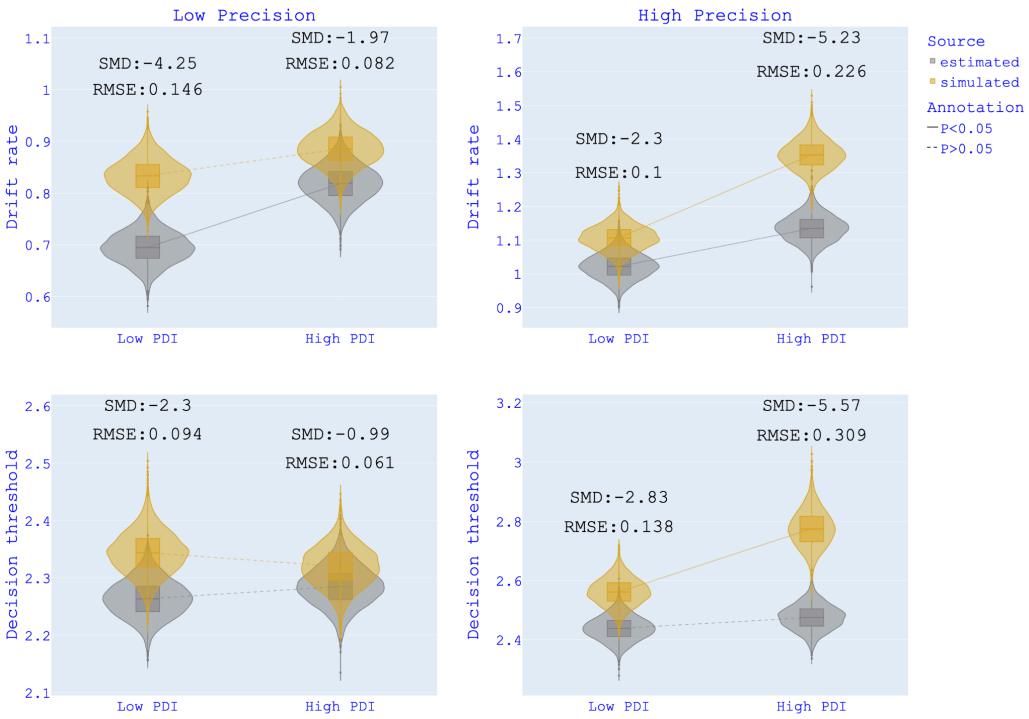

Fig.3 Parameter recovery HDDM-PDI-C. Recovery of drift rates and decision thresholds for HDDM-PDI-C (motion-coherence - PDI groups). SMD = Standardised mean difference; RMSE = Root mean squared error.

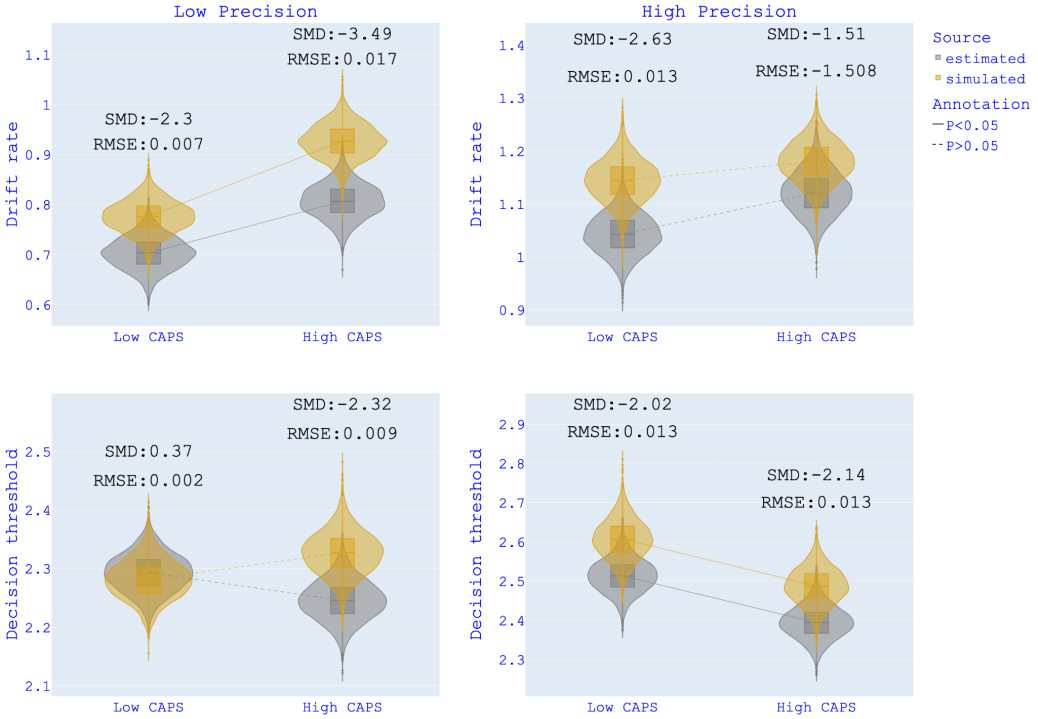

Fig.4 Parameter recovery HDDM-CAPS-C. Recovery of drift rates and decision thresholds for HDDM-CAPS-C (motion-coherence - CAPS groups).
SMD = Standardised mean difference; RMSE = Root mean squared error.

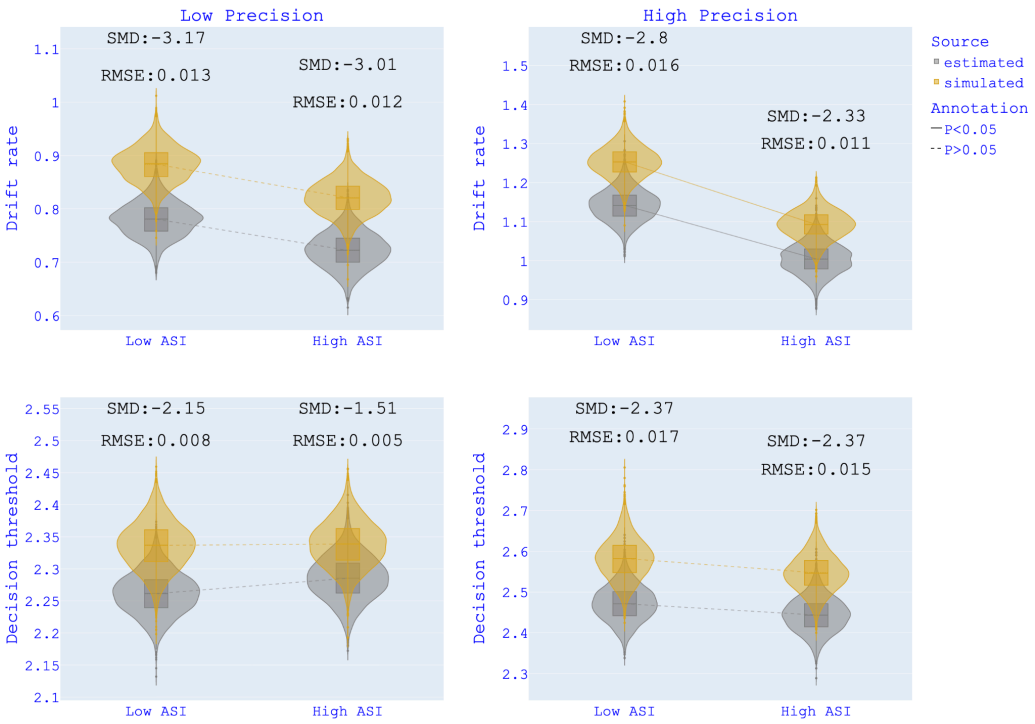

Fig.5 Parameter recovery HDDM-ASI-C. Recovery of drift rates and decision threshold for HDDM-ASI-C (motion-coherence - ASI groups). SMD = Standardised mean difference; RMSE = Root mean squared error.

Regression HDDMs

For regression HDDMs, the mean RMSE is 0.192 s for correct responses and 0.625 s for error responses (see *Figure 6*).

When predicting drift rate, regression models show a general underestimation of β coefficients for PDI, CAPS and ASI (*Figure-7* top). This underestimation affected the recovery of the effect of PDI and CAPS and produced in the simulation model a significant negative effect of ASI where there was no detectable effect in the empirical model. The recovery of the β coefficient was more precise when predicting decision thresholds, at least for CAPS and ASI (*Figure 6*-bottom). The simulated estimate for CAPS produced a pattern not reaching significance but compatible with the negative effect of CAPS on decision threshold present in the empirical model (*Figure 8* bottom-centre).

For the effect of motion-coherence, both the effects on drift rate and decision threshold were well recovered in all models. The effects of psychotic phenotypes (PDI, CAPS, ASI) on DDM parameters were better recovered in the between-group models than in the regressions. However, overall, the RT predictions of regression HDDMs were as good ad the ones from between-group HDDMs, which led us to report results form both modelling approaches.

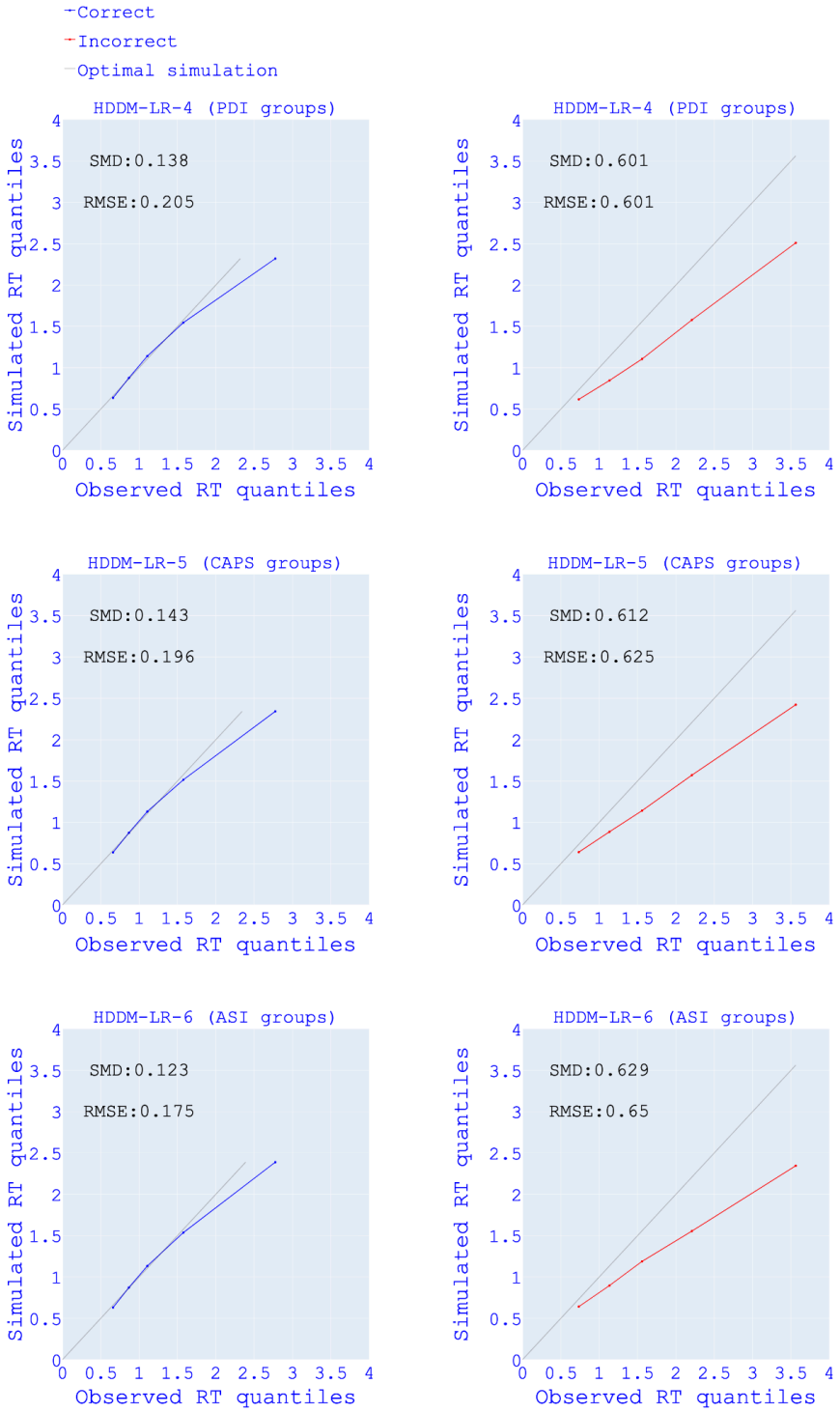

Fig.6 RT predictions of regression HDDMs Study 1. Linearity plots of observed reaction time (RT) quantiles (x-axis) and simulated RT quantiles (y-axis) for correct and error responses of regression models in *Study 1*. SMD = Standardised mean difference; RMSE = Root mean squared error.

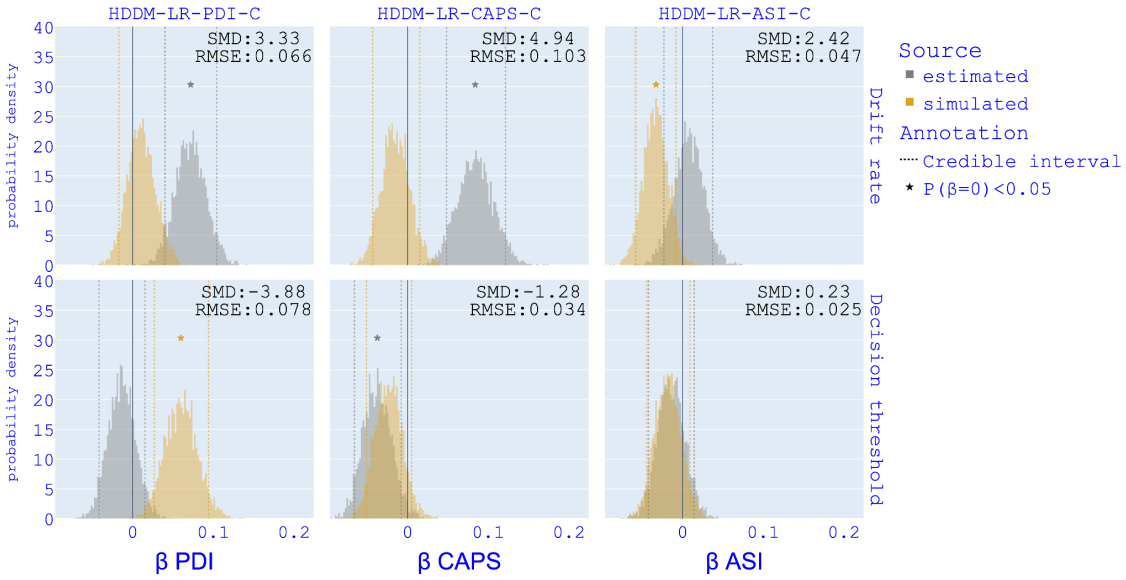

Fig. 7. Parameter recovery for psychotic phenotype HDDM-LR-PDI-C, HDDM-LR-CAPS-C ,HDDM-LR-ASI-C . Recovery of β for Schizotopy in HDDM-LR-PDI-C (motion-coherence - PDI groups), HDDM-LR-CAPS-C (motion-coherence - CAPS groups), HDDM-LR-ASI-C (motion-coherence - ASI groups). SMD = Standardised Mean Difference; RMSE = Root mean squared error.

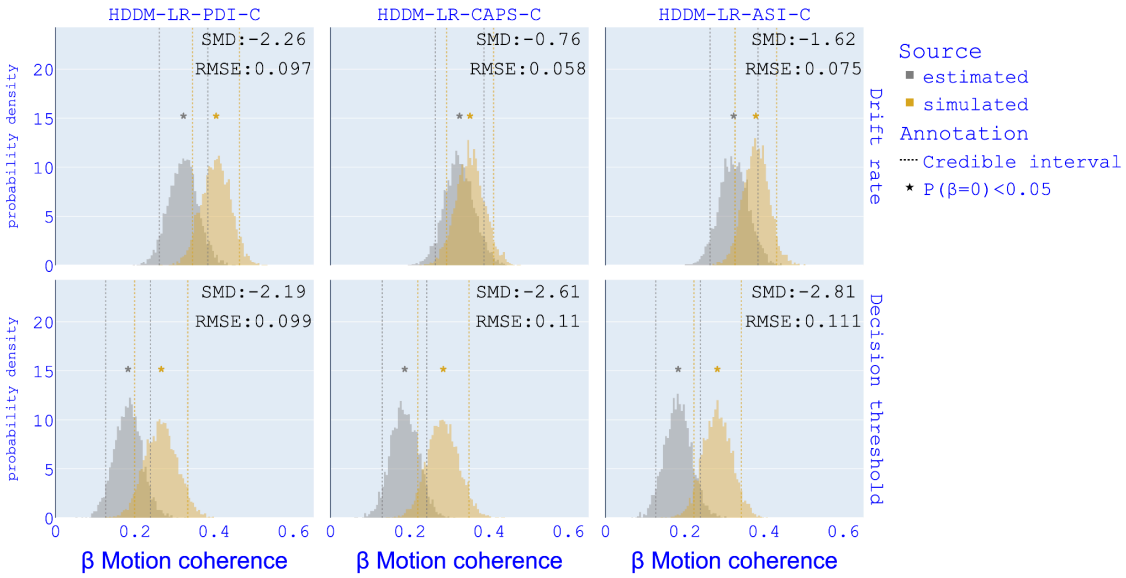

Fig. 8. Parameter recovery for motion-coherence HDDM-LR-PDI-C, HDDM-LR-CAPS-C, HDDM-LR-ASI-C . Recovery of β for motion-coherence in HDDM-LR-PDI-C (motion-coherence - PDI groups), HDDM-LR-CAPS-C (motion-coherence - CAPS groups), HDDM-LR-ASI-C (motion-coherence - ASI groups). SMD = Standardised Mean Difference; RMSE = Root mean squared error.

2.3 Discussion

We performed data simulation and parameter recovery of the HDDMs and evaluated to what extent our models were able to capture the hidden causes that produced our data. We specifically looked at whether our models were able to simulate the empirical data and recover within the simulated sample the effects identified in the empirical models. We recognised five common patterns that we will comment on before going into the specifics of the models.

(1) From the comparison between simulated and empirical RT quantiles, we notice a systematic difference in models' predictions for correct and error responses. In fact, in simple perceptual decision-making tasks (as the RDM), correct responses outnumber to a great extent error responses, as exemplified by the RT distribution in *Figure-1* With more data available, the models were hence better at predicting RT for correct responses than for error responses. In future experiments, the collection of larger samples might improve predictions of RT for error responses.

(2) Generally, the models underestimated RTs. This prediction error is mainly driven by an underestimation of slow RTs and increases for slower RTs (see *Figure 10*).

(3) Between-group models overestimated drift rates. This overestimation seems to be a systematic bias of the models that affected median-split groups uniformly and did not prevent the good recovery of the effects of grouping on the parameter. This overestimation might have produced in the simulated data the aforementioned underestimation of RTs, as RTs are inversely related to the drift rate.

(4) In some cases, effects that were only trends in the empirical data resulted significant in the simulated model (specifically for differences between high- and low-PDI groups in high coherence; see *Figure-3* right). In a few cases, the simulation models produced what we can call "synthetic false positives", meaning significant effects that were not present in the empirical models. These synthetic false positives could potentially indicate a lack of reliability in the null effects found in the empirical models, but it is uncertain if they can represent actual false negatives in the empirical results.

Although drift rates have been generally overestimated by the models, the simulations reproduced the differences on drift rate between the median-split groups present in the empirical data and reported in the *Results* section. Simulated estimates of decision threshold were also generally higher than the empirical estimates. This overestimation did not prevent the recovery of the negative effect of CAPS.

Regression HDDMs were as good as between-group HDDMs at predicting empirical RTs (see *Figure 2* and *Figure 6*) and recovered quite precisely all the effects of motion-coherence on DDM parameters. Nevertheless, regression HDDMs showed a less accurate recovery of the effects of psychotic phenotypes. In fact, only the negative effect of CAPS on the decision threshold has been fully recovered. The failed recovery of the psychotic phenotype effect on drift rates in regression HDDM presents us with a scenario where we see two types of models, the between-(median-split)-group and regression HDDMs, where the same positive effects of PDI and CAPS on drift rate were detected in the empirical data in both type of HDDM but were in one case well recovered (between-group HDDMs) but not in the other (regression HDDMs). This suggests that a positive association between drift rate and psychotic phenotype is present in the data but is better captured by models that make the parameter vary between median-split groups rather than linearly. This model comparison may open an interesting question about information processing alterations within the psychosis continuum. It is, in fact, possible that the precision of sensory evidence (proxied here by drift rate) in perceptual inference does not increase linearly with psychotic phenotypes in the general population, but only after a threshold (in our studies the median of PDI and CAPS).

3. Results of preregistered analysis

HDDM. We report here the results from hierarchical drift-diffusion models (HDDMs) we preregistered. The models we preregistered assessed the effect of the psychotic phenotype on drift rate and decision threshold in trials involving only one motion-coherence condition. However, these models could not account for within-participant variability across different motion-coherence conditions, potentially leading to less precise parameter estimations compared to models we presented in the paper that accounted for both motion-coherence and psychotic phenotype effect.

The preregistered models showed results consistent with the ones we presented in the main body of the paper. Drift rate showed to be significantly higher for high-PDI and high-CAPS groups respectively compared to low-PDI and low-CAPS groups in both motion-coherence conditions (see Fig.1-A and -C). The high-ASI group showed a significantly lower drift rate compared to the low-ASI group in the 25% motion-coherence condition (see Fig.1-A). The decision threshold for the high-CAPS group was shown to be lower than one for the low-CAPS group in the 25% motion-coherence condition (see Fig.1-B).

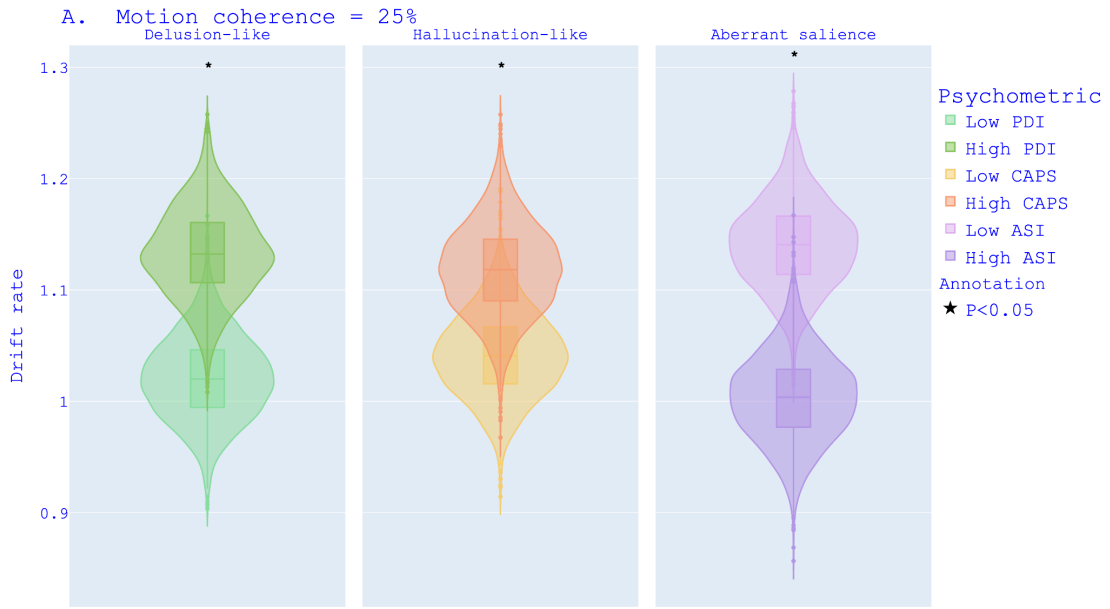

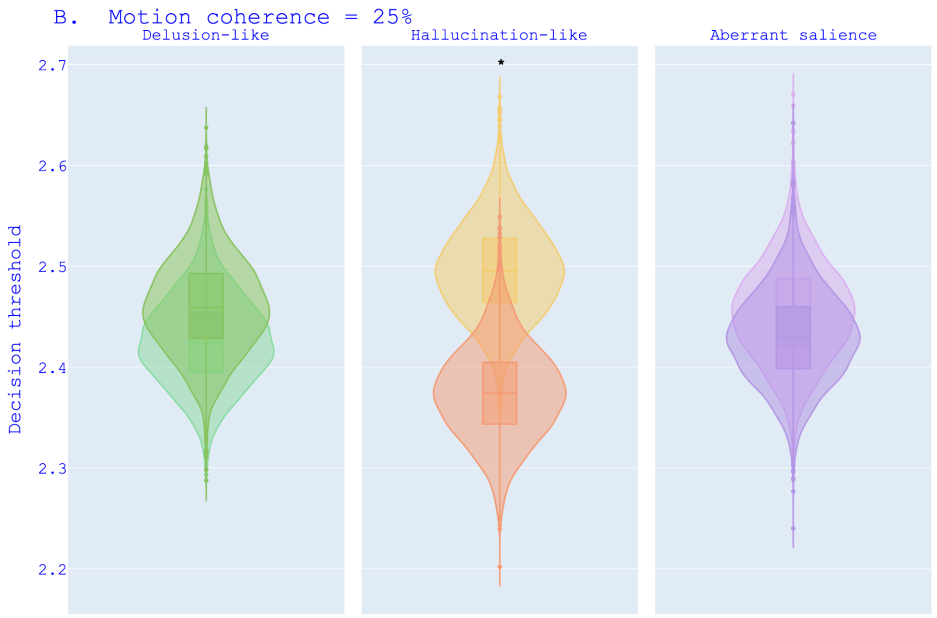
B. Motion coherence = 25%
Delusion-like
Hallucination-like
Aberrant salience
Decision threshold
2.7
2.6
2.5
2.4
2.3
2.2
*

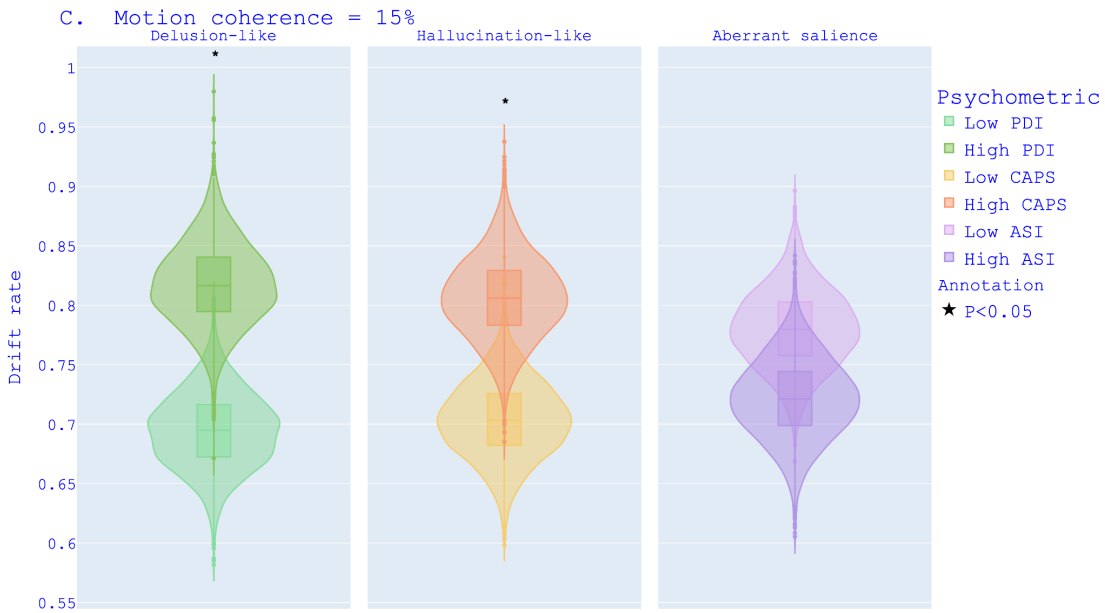
C. Motion coherence = 15%
Delusion-like
Hallucination-like
Aberrant salience
Drift rate
1
0.95
0.9
0.85
0.8
0.75
0.7
0.65
0.6
0.55
*
*
Psychometric
Low PDI
High PDI
Low CAPS
High CAPS
Low ASI
High ASI
Annotation
★ P<0.05

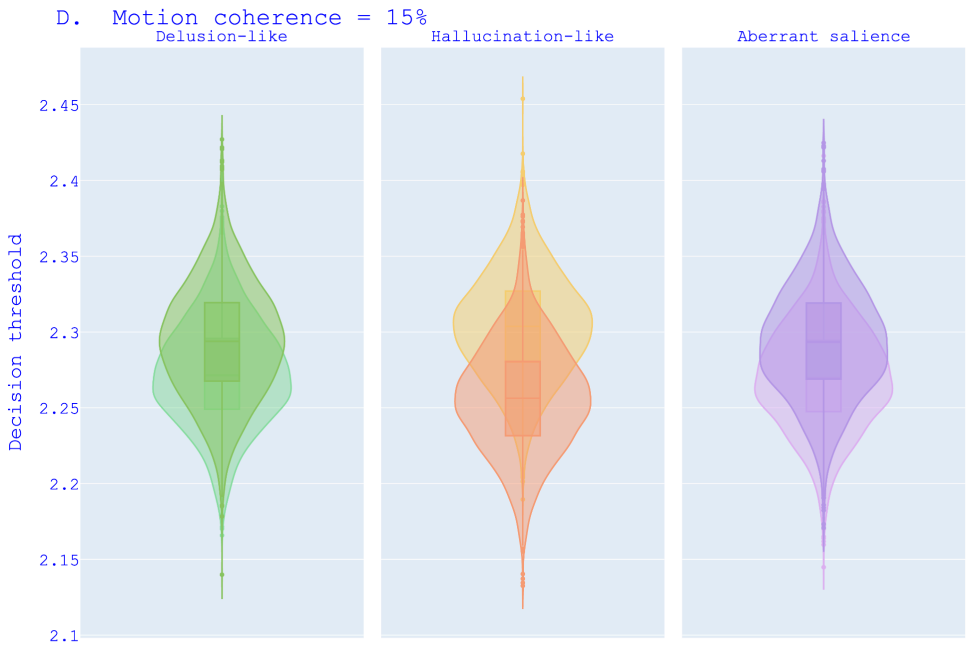

Fig 1. Between-group comparison of preregistered HDDMs. Posterior probability density distributions of drift rate (A) and decision threshold (B) in the 25% motion-coherence condition and drift rate (C) and decision threshold (D) in the 15% motion-coherence condition for median-split groups of psychotic phenotypes. Bold lines and adjacent annotations indicate the means of the distributions.

Linear regression. Here, we show the results from the ordinary least squares models we preregistered (see *Fig 2*). Because of the violation of the assumption of normal distribution of outcome variables, we did not include them in the main body of the paper.

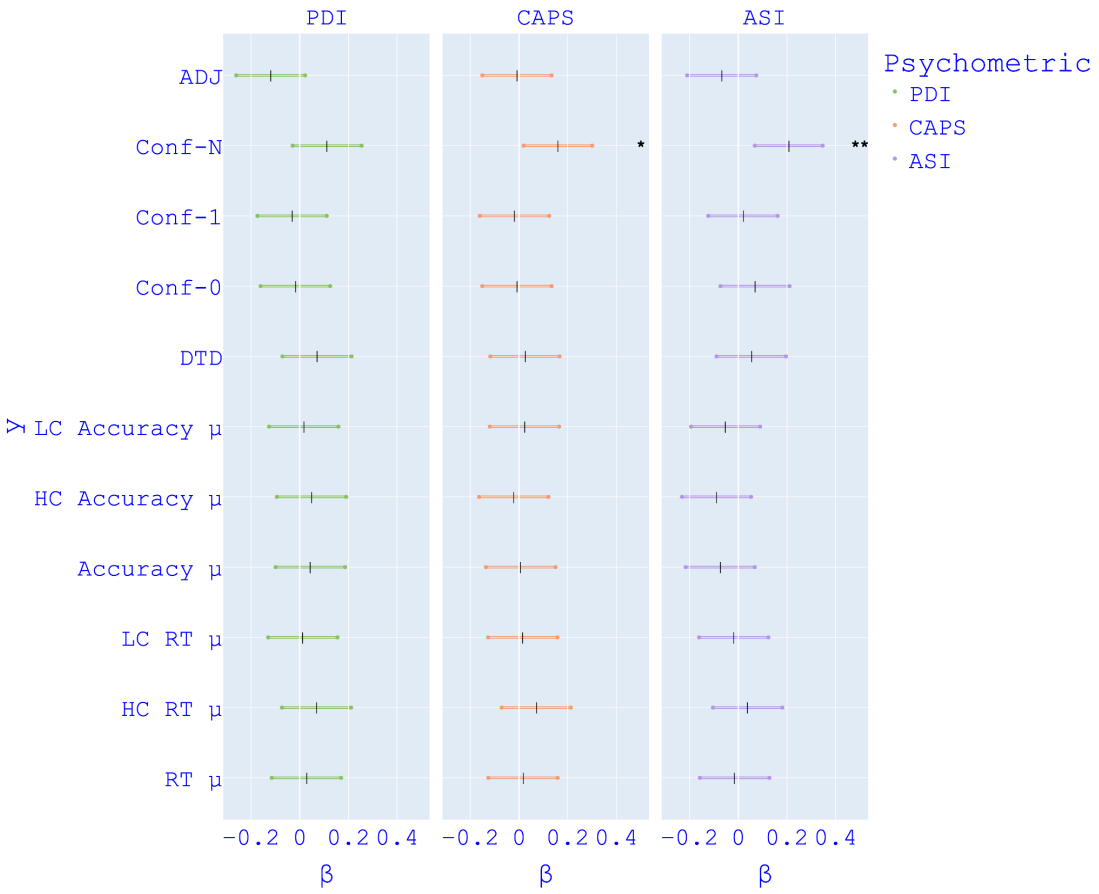

Fig 2. OLS regression models. Results from ordinary least squares models, each with PDI, CAPS and ASI as the predictor. Vertical dashes indicate the estimates for β and coloured points the upper and lower bounds.

HC=High motion-coherence
LC=Low motion-coherence
RT=Reaction time
DTD=Draws to decisions

Conf-0= Confidence at 0 draws
Conf-1= Confidence at the first draw
Conf-N= Confidence at the last draw
ADJ = Belief adjustment

*p<0.05

**p<0.01

References

Davies, D. J., Teufel, C., & Fletcher, P. C. (2018). Anomalous Perceptions and Beliefs Are Associated With Shifts Toward Different Types of Prior Knowledge in Perceptual

Inference. *Schizophrenia Bulletin*, *44*(6), 1245–1253. https://doi.org/10.1093/schbul/sbx177

O'Callaghan, C., Hall, J. M., Tomassini, A., Muller, A. J., Walpola, I. C., Moustafa, A. A., Shine, J. M., & Lewis, S. J. G. (2017). Visual Hallucinations Are Characterised by Impaired Sensory Evidence Accumulation: Insights From Hierarchical Drift Diffusion Modeling in Parkinson's Disease. *Biological Psychiatry: Cognitive Neuroscience and Neuroimaging*, *2*(8), 680–688. https://doi.org/10.1016/j.bpsc.2017.04.007

Vandekerckhove, J., & Tuerlinckx, F. (2007). Fitting the ratcliff diffusion model to experimental data. *Psychonomic Bulletin & Review*, *14*(6), 1011–1026. https://doi.org/10.3758/BF03193087

Wiecki, T. V., Sofer, I., & Frank, M. J. (2013). HDDM: Hierarchical Bayesian estimation of the Drift-Diffusion Model in Python. *Frontiers in Neuroinformatics*, *7*, 14. https://doi.org/10.3389/fninf.2013.00014

Wilson, R. C., & Collins, A. G. (2019). Ten simple rules for the computational modeling of behavioral data. *eLife*, *8*, e49547. https://doi.org/10.7554/eLife.49547